

(19)



Europäisches Patentamt
European Patent Office
Office européen des brevets



(11) Publication number:

0 364 879 A3

(12)

EUROPEAN PATENT APPLICATION(21) Application number: **89118950.8**(51) Int. Cl.⁵: **H01L 27/06, G11C 27/02**(22) Date of filing: **12.10.89**(30) Priority: **17.10.88 US 259027**(43) Date of publication of application:
25.04.90 Bulletin 90/17(84) Designated Contracting States:
AT BE CH DE ES FR GB GR IT LI LU NL SE(86) Date of deferred publication of the search report:
30.12.92 Bulletin 92/53(71) Applicant: **STANFORD UNIVERSITY**
857 Serra Street, Second Floor
Stanford, CA 94305-6225(US)

(72) Inventor: **Marsland, Robert A.**
134 D Escondido Village
Stanford, CA 94305(US)
Inventor: **Rodwell, Mark**
7931 Rio Vista Street
Goleta, CA 93117(US)
Inventor: **Bloom, David M.**
140 Golden Oak Drive
Portola Valley, CA 94025(US)

(74) Representative: **Sparing - Röhl - Henseler**
Patentanwälte
Rethelstrasse 123 Postfach 14 02 68
W-4000 Düsseldorf 1(DE)

(54) **Gallium arsenide monolithically integrated sampling head using equivalent time sampling having a bandwidth greater than 100 GHz.**

(57) A high bandwidth RF sampler using equivalent time sampling comprising an RF coplanar waveguide integrated with sampling diodes on a gallium arsenide substrate. A monolithic, integrated nonlinear transmission line is integrated on the same substrate to receive sample pulses. These pulses are reshaped by the nonlinear transmission line to have a very fast edge. This edge is differentiated by a shunt inductance of a short circuit termination of a slot line portion of the RF signal coplanar waveguide. The resulting delta function sample pulses cause the sample diodes and integrated capacitors to develop an intermediate output frequency which is a replica of the RF signal at a lower frequency and no voltage conversion loss. RF signals of up to 300 GHz can be sampled using this circuit.

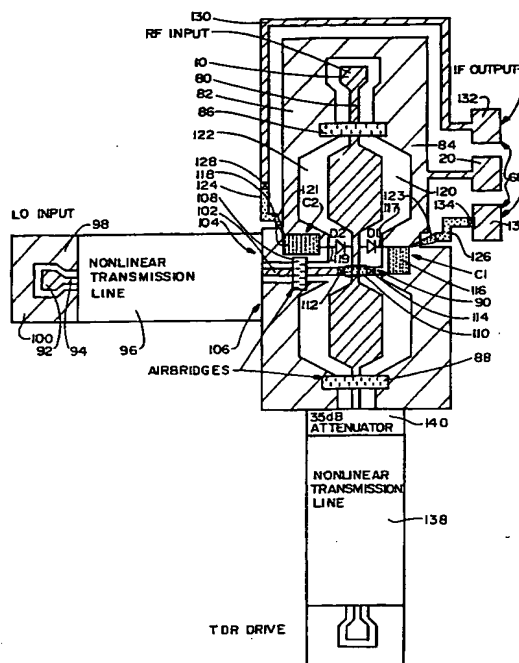


FIG. 5

**Application Number**

EP 89 11 8950

DOCUMENTS CONSIDERED TO BE RELEVANT			CLASSIFICATION OF THE APPLICATION (Int. Cl.5)
Category	Citation of document with indication, where appropriate, of relevant passages	Relevant to claim	
D, Y	EP-A-0 180 562 (TELEFONAKTIEBOLAGET L M ERICSSON) 7 May 1986	1-4, 12	H01L27/06 G11C27/02
A	* page 2, line 31 - page 5, line 16; claims 1-2; figures 1-4 *	5-6, 9-11, 13	
Y	ELECTRONICS LETTERS vol. 24, no. 2, 21 January 1988, ENAGE GB pages 100 - 101 M. J. W. RODWELL ET AL. 'Generation of 7.8 ps electrical transients on a monolithic nonlinear transmission line'	1-4, 12	
A	* the whole document *	13	
Y	PATENT ABSTRACTS OF JAPAN vol. 012, no. 150 (E-606) 10 May 1988 & JP-A-62 264 723 (YOKOGAWA ELECTRIC CORP) 17 November 1987 * abstract *	1-4, 12	
			TECHNICAL FIELDS SEARCHED (Int. Cl.5)
			H01L G11C H03K
The present search report has been drawn up for all claims			
Place of search THE HAGUE		Date of completion of the search 29 OCTOBER 1992	Examiner FRANSEN L.J.L.
CATEGORY OF CITED DOCUMENTS		T : theory or principle underlying the invention E : earlier patent document, but published on, or after the filing date D : document cited in the application L : document cited for other reasons ----- & : member of the same patent family, corresponding document	
X : particularly relevant if taken alone Y : particularly relevant if combined with another document of the same category A : technological background O : non-written disclosure P : intermediate document			

(19)



Europäisches Patentamt
European Patent Office
Office européen des brevets

(11) Publication number:

0 364 879
A2

(12)

EUROPEAN PATENT APPLICATION

(21) Application number: 89118950.8

(51) Int. Cl.⁵: H01L 27/06 , G11C 27/02

(22) Date of filing: 12.10.89

A request for correction of the reference numerals throughout the description has been filed pursuant to Rule 88 EPC. A decision on the request will be taken during the proceedings before the Examining Division (Guidelines for Examination in the EPO, A-V, 2.2).

(30) Priority: 17.10.88 US 259027

(43) Date of publication of application:
25.04.90 Bulletin 90/17(54) Designated Contracting States:
AT BE CH DE ES FR GB GR IT LI LU NL SE(71) Applicant: STANFORD UNIVERSITY
350 Cambridge Avenue Suite 200
Palo Alto, CA 94306(US)

(72) Inventor: Marsland, Robert A.
134 D Escondido Village
Stanford, CA 94305(US)
Inventor: Rodwell, Mark
7931 Rio Vista Street
Goleta, CA 93117(US)
Inventor: Bloom, David M.
140 Golden Oak Drive
Portola Valley, CA 94025(US)

(74) Representative: Sparing - Röhl - Henseler
Patentanwälte
Rethelstrasse 123 Postfach 14 02 68
D-4000 Düsseldorf 1(DE)

(54) Gallium arsenide monolithically integrated sampling head using equivalent time sampling having a bandwidth greater than 100 GHz.

(57) A high bandwidth RF sampler using equivalent time sampling comprising an RF coplanar waveguide integrated with sampling diodes on a gallium arsenide substrate. A monolithic, integrated nonlinear transmission line is integrated on the same substrate to receive sample pulses. These pulses are reshaped by the nonlinear transmission line to have a very fast edge. This edge is differentiated by a shunt inductance of a short circuit termination of a slot line portion of the RF signal coplanar waveguide. The resulting delta function sample pulses cause the sample diodes and integrated capacitors to develop an intermediate output frequency which is a replica of the RF signal at a lower frequency and no voltage conversion loss. RF signals of up to 300 GHz can be sampled using this circuit.

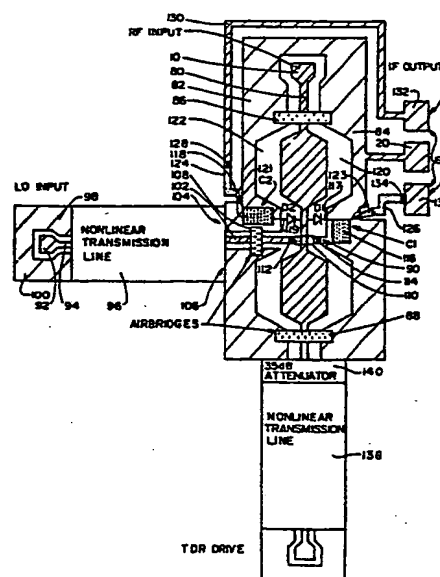


FIG. 5

EP 0 364 879 A2

The invention pertains to the field of sampling very high frequency RF signals. More specifically, the invention relates to an integrated sample head which uses equivalent time sampling for generation of an intermediate frequency output signal which is an equivalent time replica of the RF input signal to be sampled.

In the prior art, thin film signal samplers have been made in several different forms. In the earliest form, the signal samplers were brass blocks with holes machined therein with suspended center conductor to act as waveguides. One hole was used as a waveguide for the RF signal to be sampled and another hole was used to guide the sample pulses used to turn on the sample gate. The difficulty with these sampling devices was that the frequency at which they could operate was limited by the smallest diameter hole which could be machined into the brass block. The diameter of each waveguide defines the upper frequency at which the waveguide was useful.

A later version of prior art signal sampler design involved hybrid assemblies of discrete components. In this type of device, discrete diodes and thin film quartz substrate technology with integrated planar waveguides was used. U.S. patent 4,672,341 is representative of this technology. The difficulty with this approach was that integration on the substrate was on both sides with an integrated waveguide on the front side bringing the sample pulse in and an integrated waveguide on the back side bringing in the RF signal to be sampled. The structure of the device also involved a third layer microstrip. The RF signal to be sampled was guided through a via hole to the diodes on the top side of the substrate. This via hole caused extra parasitic inductance in the signal path and put a limit on the bandwidth for the signal sampler.

Performance of these hybrid structures was limited by how well the three layer structure could be fabricated and aligned as well as the intrinsic limitations caused by the spatial separation of the sample pulse generating structure from the sampling diodes. At frequencies in the range of hundreds of GHz, with signals traveling at approximately one-third the speed of light along the waveguides, even the smallest spatial separation between devices can cause losses and dispersion, and results in parasitic components which limit the bandwidth. Therefore, even a 100 micron misalignment in fabrication of such a structure translates to a one picosecond penalty. Since the desired aperture time is less than 5 picoseconds for a large bandwidth, such misalignment errors can substantially adversely affect the bandwidth by rendering it impossible to get a fast edge to the differentiator to generate a very short sample pulse. To get a fast edge to the differentiator, it is necessary to

have very close spatial proximity between the structure which generates the short sample pulses and the signal line carrying the signal to be sampled.

An attempt at improving the hybrid structure is found in the latest generation of Hewlett Packard's signal samplers dating from February of 1986. In this latest generation of signal samplers, integrated gallium arsenide diodes are used for sampling the RF signal. Beam leads couple these diodes to step recovery diodes which generate the sample pulses which turn the gallium arsenide diodes on. The pulse generator, however, is not integrated on the same substrate with the differentiator because prior to the invention described herein, it is believed that no workers in the art were in possession of a gallium arsenide pulse generator of a monolithic design. In the Hewlett Packard design, integrated diodes, resistors, and capacitors are formed on the gallium arsenide substrate. These integrated components are connected by beam leads bonded to pads on the substrate to make connection to the other elements of the sampler circuit. The nonintegrated structures are a differentiating line to differentiate the voltage steps from the step recovery diodes to generate the sample pulses used to turn on the gallium arsenide diodes, and a microstrip line integrated on another substrate. Thus, the Hewlett Packard design requires at least two substrates with connections between them. This spatial separation between the pulse generation circuitry and the sampling diodes causes losses, dispersion, and parasitics which limit the bandwidth of the sampler.

It is highly desirable in many applications to work with RF signals having very high frequencies such as 300 GHz. To be able to see these signals on low frequency oscilloscopes for analysis, testing, and other purposes, it is necessary to down convert them to a lower frequency. One way of doing this is to sample these signals to generate a replica signal at a lower frequency which is within the range of frequencies which can be observed on commercially available oscilloscopes. To do this requires a very high bandwidth signal sampler which can generate sample pulses to turn on the sampling diodes having a pulse width on the order of less than 2 picoseconds. This requires precise control of dimensions and close proximity of all elements such as can be obtained in fully integrated, planar structures.

Therefore, a need has arisen for a signal sampler with a fully integrated monolithic design wherein spatial separation between the pulse generator and the sampling diodes is minimal, and wherein dimensional controls can be very exact.

Summary of the Invention

According to the teachings of the invention, there is taught a fully integrated, monolithic signal sampler formed on a gallium arsenide substrate using conventional planar processing.

The gallium arsenide substrate is layered by molecular beam epitaxy to have buried N^+ layer beneath an N^- layer. On this gallium arsenide substrate there is fabricated a pulse generator in the form of a nonlinear transmission line in the form of a coplanar waveguide. This device shapes sample pulses received from a local oscillator. These sample pulses, when they arrive at the input on the nonlinear transmission line, have a first rise time (or fall time depending upon the convention chosen) which is altered as the sample pulses propagate down the nonlinear transmission line. The sample pulses propagate along the nonlinear transmission line toward the locations of a pair of gallium arsenide, integrated sample diodes. As the sample pulses propagate down the coplanar waveguide nonlinear transmission line, the rise time of the sample pulses is substantially shortened to less than 5 picoseconds for the sample pulses emerging from the nonlinear transmission line.

Another coplanar transmission line is integrated on the same substrate and receives at its input the RF signal to be sampled. This RF signal can have a frequency of up to 300 GHz in the preferred embodiment. The sampling diodes are coupled to the RF transmission line in a balanced, antiparallel relationship to maintain isolation between the RF and the input port and output port.

The sample pulses emerging from the nonlinear transmission line, hereafter called intermediate pulses, are differentiated to generate a series of delta function sample pulses. These delta functions have a pulse width which is approximately equal to the rise time of the intermediate sample pulses. As each intermediate pulse arrives, it turns on the sample diodes. Differentiation is accomplished by coupling the intermediate sample pulses to a slot line acting as a shunt inductor. The slot line is a pair of shorted sections of the RF signal coplanar waveguide. The coplanar waveguide of the nonlinear transmission line is coupled only to the two ground planes of the RF signal coplanar waveguide through a 50 ohm termination and excites the slot line mode of propagation therein. The intermediate sample pulses propagate in slot line mode in two directions away from the point of coupling between the nonlinear transmission line and the RF signal coplanar waveguide. Propagation in each direction continues until an air bridge termination shorting the two ground planes is encountered in each direction. These short circuit terminations cause reflection of the sample pulses back toward the

point of injection.

As each intermediate pulse arrives back at the point of injection into the ground planes of the RF coplanar waveguide, it turns off the pair of integrated gallium arsenide sampling diodes. These diodes are coupled through integrated capacitors to the ground planes of the RF signal coplanar waveguide. These sample diodes are integrated adjacent to the position of injection of the intermediate pulses into the RF coplanar waveguide.

The dimensions of the slot line portion of the RF coplanar waveguide are established such that the round trip travel time is approximately equal to the rise time of the intermediate sample pulses and the characteristic impedance is 78 ohms to match the characteristic impedance of the nonlinear transmission line for development of maximum voltage across the diodes as possible.

An integrated resistor formed in the N^+ layer of the gallium arsenide substrate couples the nodes between each of the sampling diodes and the associated integrated capacitor. A center tap on this integrated resistor serves as the output node for the system from which the intermediate frequency (IF) sampled signal can be extracted. This IF signal is a replica of the RF signal in that it has the same voltage at points of corresponding phase as the voltage of the RF signal but the IF signal has a frequency which is substantially less than the RF signal frequency.

Brief Description of the Drawings

Figure 1 is a schematic diagram of the sample head of the invention.

Figure 2 is a diagram illustrating equivalent time sampling.

Figure 3 is a block diagram of a nonlinear transmission line.

Figures 4(a) and 4(b) are illustrations of the input sample pulse to the nonlinear transmission line and the output intermediate pulse therefrom.

Figure 5 is a plan view of the layout of the integrated sampling circuit according to the teachings of the invention.

Figure 6(a) is a circuit diagram of the sampling diodes laid out to correspond to the cross-section of the sampling diode structure shown in Figure 6(b).

Figure 6(b) is a cross-section of the diode and RF waveguide structure shown in plan view in Figure 6(c).

Figure 6(c) is a plan view of the sampling diode and RF waveguide structure.

Figure 6(d) is a cross-sectional view of a sampling diode.

Figure 7 is a partial plan view of the in-

egrated sample head showing the interconnections of the diodes, capacitors, resistors and coplanar waveguides which are combined to implement the circuit of Figure 1.

Figure 8 is an illustration of a fast edge which was sampled using a sample head having the construction of Figure 7.

Figure 9 is schematic diagram of a nonlinear transmission line.

Figure 10 is a cross sectional view of the structure of a nonlinear transmission line according to the teachings of the invention taken through a diode isolation island.

Figure 11 is a diagram of the input signal and the output signal from the nonlinear transmission line of the invention showing the results of the compression.

Figure 12 is a plan view of the structure of the invention.

Figure 13 is a plan view of the outline of the isolation implant mask.

Figure 14 is a plan view of the diode, including diode contact region and ohmic contact regions.

Figure 15 is a cross sectional view of the structure during an intermediate stage of device construction during formation of the ohmic contacts.

Figure 16 is a cross sectional view of the structure of the device during the isolation implantation.

Figure 17 is a diagram of the relative wave shapes of the input and output signals from the transmission line according to the teachings of the invention as implemented in a scale model of the preferred embodiment.

Figure 18 is a cross sectional view of another embodiment of the invention through the diode area.

Figure 19 is a cross sectional view of another embodiment of the invention through a region outside the diode isolation island.

Figure 20 is a schematic plan view of an embodiment of the invention wherein the diode junction areas are successively smaller and the spacing between diodes becomes progressively smaller.

Figure 21 is a cross sectional view of the diode region of another embodiment of the invention.

Figure 22 is a cross sectional view of the diode region of another embodiment of the invention.

Figure 23 is a schematic cross sectional view of another embodiment of the invention.

Figure 24 a cross sectional diagram of the preferred embodiment of the nonlinear transmission line.

Detailed Description of the Preferred Embodiment

Referring to Figure 1, there is shown a schematic diagram of the signal sampler which is implemented in integrated form according to the teachings of the invention. The circuit of Figure 1 receives a high frequency RF signal to be sampled at an RF port 10. A local oscillator port 12 receives local oscillator sample pulses, usually sawtooth in shape, at a frequency such that the n_{th} harmonic of the local oscillator frequency is offset from the fundamental frequency of the periodic RF signal to be sampled by a frequency Delta. The local oscillator pulses are differentiated by a shunt inductance symbolized by the impedances Z1 and Z2, 14 and 16, respectively in Figure 1. These shunt inductances are implemented by a short-circuited section of a slot line portion of the coplanar waveguide serving to guide the RF signal to be sampled and will be described in more detail below. The slot line guides the sample pulses to the location of an air bridge short circuit termination where they are reflected back toward nodes 56 and 57. The resultant voltage between nodes 56 and 57 is the derivative of the sample pulse. The sample pulse propagates along the slot line in the even mode whereas the RF propagates along the coplanar waveguide in the odd mode thereby minimizing coupling between the two signals.

The sample pulses appearing across nodes 56 and 57 turn on diodes D1 and D2 each time a sample pulse occurs. Because the RF signal is offset from the n_{th} harmonic of the local oscillator frequency by the frequency Delta, the sample pulses will sample the RF wave form once every n cycles. There results an output signal at an intermediate frequency at an intermediate frequency (IF) output port 24. This sampling process is illustrated in Figure 2.

In Figure 2, the wave form 22 represents the output signal at the intermediate output port 24 in Figure 1. The points marked 26, 28, 38, 40, 42 and 44 are typical sample points, and correspond, respectively, to the points 30, 32, 46, 48, 50 and 52 on the RF wave form 34. The wave form 34 is the signal to be sampled and must be periodic.

The impulses shown at 36 represent the differentiated sample pulses, and are termed Delta functions. The sample pulses occur at a repetition rate of f_0 which is the local oscillator (LO) frequency. Delta functions are the most desirable form of sample pulse to use because the harmonic amplitude of a Delta function pulse is level throughout the harmonic spectrum. This allows a broader range of RF frequencies to be sampled without voltage conversion loss. The integrated nonlinear transmission line allows the rise time of the incoming sample pulses to be substantially shortened.

When this fast edge is differentiated, a sampling pulse results which has a pulse width which is substantially equal to the rise time of the fast edge. Since this pulse width can be anywhere from 7.8 picoseconds to 1.5 picoseconds, an approximation of a true Delta function having a pulse width substantially near 0 can be achieved with the integrated, monolithic structure of the invention.

Inspection of Figure 2 shows how the occurrence of the sampling pulses corresponds to the sample points on the RF wave form 34 and the corresponding points on the wave form shown at 22. The sampled output wave form occurs at a frequency of Delta. Note also that the voltage at the sample point 26 corresponds to the voltage of the RF wave form at sample point 30 while the voltage at the sample point 28 corresponds to the voltage of the RF sample waveform 34 at point 32. Likewise, the sample voltage at points 38, 40, 42, and 44 correspond, respectively, to the voltage at the points 46, 48, 50, and 52 on the RF waveform 34.

The manner in which this sampling is accomplished is as follows. Referring to Figure 1, consider the case where the RF is off such that no RF signal 34 appears at the port 10. Assume that the local oscillator is turned on at time $T=0$ and that intermediate sample pulses such as the pulse shown at 54 begin arriving at the node 56. The current resulting from each intermediate sample pulse travels along the path 58 through the inductance segments Z1 and Z2 representing the inductance of the slot line portion of the RF coplanar waveguide. It can be shown from network theory that the voltage at node 56 is equal to the derivative of the input voltage at the local oscillator port 12 times a constant equal to the round trip inductance of the short circuited slot line path divided by the resistance in series with the path.

Note that the intermediate sample pulse 54 has a one edge which is much shorter than the other edge. It is the differentiation of this sharp rise time which causes the Delta function sample pulses shown at 36 in Figure 2. The first sample pulse is at least two volts and therefore turns both diodes D1 and D2 on hard for the duration of the sample pulse. When the pulse is over, a large amount of current has passed in the forward direction through capacitors C1 and C2, but very little current has passed through them in the reverse direction. This leaves a charge Q on capacitors C1 and C2, which gives rise to a voltage $Q/C1$ reverse biasing diode D1 and $Q/C2$ reverse biasing the diode D2. Because the diodes are now slightly reverse biased, the next sample pulse does not turn the diodes on quite as hard as they were turned on by the first sample pulse. However, the diodes are still forward biased by the second sample pulse which causes more charge to be left on each of the capacitors by

the end of conduction of the second sample pulse. This process continues until the reverse charge leakage through and around the diodes D1 and D2 through the resistor R1 just equals the forward charge stored during a sample pulse interval. This equilibrium condition will always occur at a fixed voltage V_r across the diodes for a given pulse amplitude and resistance R1.

Now consider the case where the RF signal is on, but the frequency of the RF is an exact harmonic frequency of the local oscillator fundamental frequency. This means that the sample pulse will always occur at the same place in each RF signal cycle. Therefore, whenever the diodes are on, the RF signal will have the same voltage at node 62 in Figure 1. The diode pair D1 and D2 will now self bias in the manner described in the previous paragraph until each diode has regained its reverse bias voltage V_r . Thus, if the voltage at node 62 is V_{RF} when the sampled pulse arrives, then the voltage at node 64 is $V_r + V_{RF}$, and the voltage at node 66 is $-V_r + V_{RF}$ in the steady state. This means that the voltage at the center tap node 68 of the resistor R1 is simply the DC value, V_{RF} .

If the fundamental frequency of the RF signal at the RF port 10 is offset from some harmonic of the local oscillator by the frequency Delta, then the sample pulses will cause sample voltages at the output node 68 that will trace out one complete RF waveform cycle in the interval $1/\Delta$ seconds. This means that the time axis of the RF signal has been scaled by a factor of f_{RF}/Δ with no voltage conversion loss in the ideal case. Thus it is seen that the final output signal at node 68 is the same as the RF input signal except it is on a scaled time axis.

In time domain instruments, it is important that the amplitudes of the RF signal harmonics be preserved as well as preserving the shape of the RF fundamental signal. Of course, if the RF signal is a sign wave, there are no harmonics. However, the signal sampler of the invention works with any periodic RF signal, and it is well known that periodic signals of a nonsine wave nature have harmonic components defined by the Fourier expansion of the time domain function representing the signal. In accordance with the teachings of the invention, sample pulses having pulse widths substantially approximating the pulse width of a Delta function are used. The result is an absence of voltage conversion loss because of the unity strength of the harmonics of the local oscillator frequency at every harmonic of interest.

There is power conversion loss in the system of the invention since the RF is being sampled for a small fraction of each cycle.

The time scale factor relating the time access of the RF signal 34 in Figure 2 and the time scale

of the sampled waveform 22 in Figure 2 is f_{RF}/f_{IF} where f_{IF} is the intermediate frequency of the output signal at node 68. This is the difference frequency between the frequency of the RF signal, f_{RF} , and the nearest harmonic of the local oscillator frequency, i.e., Delta. Real time on the time axis of the signal 34 in Figure 2 is multiplied by this scale factor to yield the equivalent time on the time axis for the signal 22 in Figure 2. If the intermediate frequency waveform is displayed on an oscilloscope, the horizontal axis of the display will be in equivalent time. Actual time is obtained by dividing by the scale factor. The process symbolized by Figure 2 is referred to as "equivalent time sampling".

Referring to Figure 3, a short summary of the operation of nonlinear transmission lines will be helpful in understanding the operation of the equivalent time sampling circuit according to the teachings of the invention. A nonlinear transmission line is a relatively high impedance transmission line which is periodically loaded with Schottky diodes serving as voltage-dependent shunt capacitances. Figure 3 is an equivalent circuit diagram for a nonlinear transmission line such as is used in the invention and Figure 4(A) shows the input pulse entering the nonlinear transmission line while Figure 4(B) shows the shape of the output pulse which emerges as a result of propagation of the input pulse down the nonlinear transmission line. The propagation delay time per section of the line is equal to the square root of the transmission line inductance times the line capacitance per section. The nonlinear capacitors make the propagation delay time a function of voltage. For the diode polarity shown in Figure 3, the diode capacitance increases with voltage so a more positive voltage on the line will have a longer delay time. This allows the more negative portions of the trailing edge of a pulse to catch up with the more positive portions of the trailing edge and the peak which shortens the rise time (or fall time depending upon perspective) of the trailing edge. Further, the voltage dependent capacitance causes the more positive peak to lag behind the more negative portions of the leading edge as is illustrated in Figure 4(B).

While the voltage dependent delay time causes one edge of an input pulse to get steeper and stretches out the other edge, dispersion on the line causes both edges to stretch out. The rise time of the pulse will therefore be reduced as the pulse propagates along such a nonlinear transmission line until, finally, the tendency of the nonlinear delay to reduce the rise time just balances the tendency of the dispersion to increase the rise time. If diode series resistance can be neglected and the diode capacitance is much larger than the capacitance per section of the line, the final limited

fall time of the pulse at the output of the nonlinear transmission line is on the order of but longer than the square root of the inductance of the line section times the capacitance per section. If the nonlinear transmission line is implemented in the form of a monolithic integrated circuit, this limiting rise time can be less than a picosecond.

Rise times of 7.8 picoseconds to 1.5 picoseconds are obtainable with today's process technology. Since the slope of the edge 70 in Figure 4(B) is negligible compared to the slope of the edge 72, the derivative of the waveform of Figure 4(B) is a narrow impulse function having a pulse width equal to the rise time of the edge 72. Hereafter, the time between the points 74 and 76 on the waveform of Figure 4(B) will be referred to as the rise time, although it can also be called the fall time.

The diode arrangement of Figure 1 is used because it allows both diodes to have the same polarity to the local oscillator. However, to the RF signal to be sampled, the diodes still appear to be anti-parallel, thus imposing only odd harmonic distortion on the RF signal. This arrangement provides natural isolation between the RF signal and the local oscillator signal since the local oscillator output is a balanced signal while the RF signal is unbalanced. Since the short circuited transmission line represented by the inductances 14 and 16 differentiate the oscillator waveform, that waveform can be a square wave or sawtooth wave rather than a series of impulses. Generation of a series of impulses by a local oscillator is possible but difficult.

Assuming that the local oscillator pulse is narrow enough, diode capacitance and series resistance directly determine the bandwidth of the sampler in two ways. First, the capacitor loading of the shunt diodes on the RF line causes the RF voltage at the diodes to have a pole in its frequency response at a frequency $1/25C1$. Thus for an RF bandwidth of 300 GHz, the capacitance of the diode loading has to be less than 10 femptofarads per diode. Second, diode capacitance and series resistance determine the turn-on time of the sampling diode. In the circuit of Figure 1, it can be shown that the turn-on time of the sampling diodes is 1.8 picoseconds (10% to 90% rise time). This rise time exists for a local oscillator source resistance of 100 ohms, a characteristic impedance of 75 ohms for the shorted slot line, a series diode resistance of 60 ohms and for the series capacitance of the two diodes equal to 5 femptofarads. This means that if the diode is biased so that it turns on at the 85% point of the applied sample pulse, and if the shorted transmission line round trip line is 4 picoseconds, that the sampling diodes will be on for 1 picosecond yielding a bandwidth of

roughly 300 GHz.

In order to achieve the high bandwidth and low values for the parasitic elements given in the previous example, it is necessary to have the local oscillator drive the sampling circuit with sufficient edge speed to develop the needed voltage across the short circuited slot line before the reflected wave returns from the short circuit termination and shuts the sampling diodes off. This means, for the design of the previous example, that the transition time or edge speed of the intermediate pulses emerging from the nonlinear transmission line must be preferably less than 4 picoseconds. By using a nonlinear transmission line to reshape the input pulse, usually a sinewave, from the local oscillator, this transition time requirement can be met. However, to couple pulses having such a fast edge speed to the local oscillator port of the sample circuit without distortion, the nonlinear transmission line must be integrated on the same chip with the sampling diodes and differentiation circuit. This means that hybrid technology and any construction technology other than full integration on the same surface of a substrate is not acceptable since the dimensional tolerances and spatial separation of these other construction options lead to losses, dispersion and parasitic loading, i.e., parasitic inductance, which would distort or destroy the fast edge speed achieved by the nonlinear transmission line.

According to the teachings of the invention, the sampling head is integrated on the same side of a substrate as a nonlinear transmission line with a single level of metallization plus air bridges. The requirement for monolithic implementation according to the teachings of the invention is quite demanding since it prohibits all prior art structures for sampling head designs which use microstrip or coax-to-slot-line local oscillator drive.

The integrated structure for the sample head according to the teachings of the invention is shown in plan view at overview scale in Figure 5. In Figure 5, the RF input port 10 consists of a conductive pad connected to a center conductor 80 of an integrated coplanar waveguide. This integrated coplanar waveguide serves to carry the RF signal to be sampled toward the sample diodes D1 and D2 shown in the middle of Figure 5. Figure 5 is intended only to show the layout of the sample head schematically and not the exact integrated structure. More detail of the exact integrated structure will be given in Figure 7.

The integrated coplanar waveguide for the RF signal is comprised of the center conductor 80 and two ground plane conductors 82 and 84. The substrate is comprised of gallium arsenide, which has an N^+ buried layer lying beneath an N^- layer both layers being formed by molecular beam epitaxy.

The doping of the N^+ layer is 3×10^{18} per cubic centimeter, while the doping of the N^- layer is 3×10^{16} per cubic centimeter. Areas underlying the RF signal integrated coplanar waveguide which need to be insulating such as most of the area between the center conductor 80 and the ground planes 82 and 84 are damaged by proton implants so as to convert the substrate in such areas into a semi-insulating material. This prevents shorting between the semiconductor and the ground plane conductors 82 and 84.

An air bridge 86 is formed to connect the ground planes 82 and 84 above the sampling diodes. Likewise, an air bridge 88 connects the two ground planes 82 and 84 at a location below the sampling diodes. These two air bridges, 86 and 88, serve as short circuit terminations for the slot line comprised of the ground plane conductors 82 and 84. These short circuit terminations cause the reflection of the incoming sample pulses propagating down the ground plane conductors 82 and 84 back toward the point of injection adjacent to the sample diodes.

The point of injection of the sample pulses is shown at 90. Input sample pulses are coupled to a contact pad 92 formed from the metal of the center electrode 94 of a nonlinear transmission line 96. The nonlinear transmission line also has two ground plane conductors 98 and 100. The structure of the nonlinear transmission line will be described in more detail below. The sample pulses are coupled into the nonlinear transmission line by coupling to the center electrode 94 via pad 92. This causes the sample pulses to propagate down the nonlinear transmission line 96 in coplanar waveguide mode. The intermediate pulses which emerge from the nonlinear transmission line are coupled into the RF signal coplanar waveguide at 90 in a manner to excite slot line propagation. That is, the center conductor 102 is coupled only to the ground plane segment 106 at point 90 and the ground plane conductors 98 and 100 of the nonlinear transmission line are coupled to the ground plane conductor 104. This applies the intermediate pulse across the slot in the RF coplanar waveguide so as to excite slot line mode propagation of the intermediate pulses toward the air bridges 86 and 88. An air bridge 108 shorts the two sections of ground plane 104 and 106 together to suppress even modes of propagation on the nonlinear transmission line and to provide continuity in the RF coplanar waveguide ground plane 82.

A buried 50 ohm resistor 110 formed in the N^+ layer of the substrate is used to terminate the coplanar waveguide carrying the intermediate sample pulses in its characteristic impedance. The center conductor 102 of the nonlinear transmission line makes an ohmic contact to the buried N^+ layer

via holes etched through the N^- layer and shown symbolically at 112 and 114. The center conductor 80 of the RF signal coplanar waveguide is coupled to an airbridge which passes over the buried 50 ohm resistor 110 to make contact with a continuation of the center conductor 80.

The entire substrate is proton implant damaged to render it semiinsulating prior to forming the waveguides thereon. Certain areas are excepted from this proton implant damage, however. Those areas include the buried path of the resistor 110 and the resistor 126, and the junction areas of the diodes D1 and D2 and all diodes of the nonlinear transmission line.

The center conductor 102 of the nonlinear transmission line is coupled through the resistor 110 to the ground plane conductor 84. The ground plane conductors 104 and 106 of the nonlinear transmission line are electrically coupled to ground plane 82 of the RF signal coplanar waveguide. As a result, the intermediate sample pulses emerging from the nonlinear transmission line 96 are coupled into the slot line mode of propagation on the RF signal coplanar waveguide at the point of injection 90. When each intermediate sample pulse arrives back at the point of injection, the sample diodes D1 and D2 are turned off thereby stopping the process of charging two integrated capacitors C1 and C2. Each of the capacitors C1 and C2 is comprised of a top plate of plated gold formed over a nitride layer which in turn is formed over a layer of evaporated Schottky metal which forms the bottom plate of the capacitor and is coincident with the ground plane conductors 82 and 84. The top plates of the capacitors C1 and C2 are shown at 116 and 118, respectively.

The resistor 110 implements the resistor labeled R2 in Figure 1. The capacitors C1 and C2 correspond to the capacitors C1 and C2 in Figure 1 and the diodes D1 and D2 correspond to the diodes D1 and D2 in Figure 1. The cathode of the diode D1 is coupled to the top plate of the capacitor C1 by an air bridge 117. The anode of the diode D1 is an extension of the Schottky metal for the center conductor 80 of the RF signal coplanar waveguide and extends out over a junction area of unimplanted N^- substrate thereby forming a Schottky diode. Likewise, the anode of the diode D2 is coupled via an air bridge 119 to the top plate 118 of the capacitor C2, while the cathode of the diode D2 is an extension of the center conductor 80 of the RF signal line and make contact to an unimplanted portion of the N^- layer via ohmic contacts to form the Schottky diode.

The resistor R1 in Figure 1 is implemented by a segment of the N^- buried layer which is masked off during the proton implant. This area is shown as two segments at 124 and 126. The area 124 is

coupled to the top plate 118 of the capacitor C2 via an air bridge 121. The air bridge 121 is coupled to the buried resistor segment 124 via an ohmic contact (not shown). The resistor segment 126 is coupled to the top plate 116 of capacitor C1 via an air bridge 123. An ohmic contact couples the air bridge to the buried resistor segment 126. The cross-sectional area and path length of the resistor segments 124 and 126 are equal such that each resistor segment has an equal resistance. The resistor segment 124 is coupled via an ohmic contact at 128 to a conductive path 130 formed on the surface of the substrate which couples the resistor segment 124 to a contact pad 132 serving as output node 68 for the IF signal. The resistor segment 126 terminates in an ohmic contact at 134 to make electrical contact to a contact pad 136 which is also, by off chip connections, the output node 68. Separate contact pads 132 and 136 allows the diodes to be separately biased slightly differently if necessary to balance the circuit.

A second nonlinear transmission line 138 is used to inject test signals into the RF coplanar waveguide for purposes of testing the bandwidth of the sampler. This nonlinear transmission line 138 is not critical to the invention and may be omitted as it is used solely for testing the performance of the sampler.

A 35 DB attenuator 140 terminates the RF signal coplanar waveguide, thereby rendering the nonlinear transmission line 138 invisible to sources of RF signals coupled to the RF input port 10.

Referring to Figures 6(A) through 6(D), there are shown further structural details of the sampling diode section of the preferred embodiment of the invention. Figure 6(A) represents the schematic diagram implemented by the structure of Figure 6-(B) which is a cross section through the sampling diode portion of the structure but not passing through the anode portions of the diode structures. Figure 6(C) is a plan view of the sampling diode and capacitor region of a structure according to the preferred embodiment of the invention. Figure 6(D) is a cross sectional diagram showing the structure of each sampling, Schottky diode. The position of the section line BB' in Figure 6(C) shows the position of the cross section of Figure 6(B). The position of the section line DD' in Figure 6(C) shows the position of the section illustrated in Figure 6(D). Figure 6(A) is the schematic diagram of Figure 1 laid out in a manner to spatially correlate to the structures shown below in Figure 6(B). Corresponding structures in Figures 6(B) and 6(D) have corresponding reference numerals.

Referring jointly to Figures 6(B), 6(C) and 6(D), further details of the sampling diode portion of the structure are given. In Figure 6(C), the diode anodes are shown as projecting fingers of Schottky

metal at 140 and 142. An active region of N+ gallium arsenide is shown outlined in phantom for each diode at 144 and 146, respectively.

The center conductor of the RF signal coplanar waveguide is shown at 80. In Figure 6(B) this is seen as a portion of the Schottky metal layer which is deposited on the surface of the proton implant damaged substrate.

The diode D1 to the right of the center conductor 80 in Figure 6(C) is illustrated in cross section in Figure 6(D). In Figure 6(D), the diode anode 142 is seen as a strip of Schottky metal placed over the active region 146 between two ohmic contacts 148 and 150 which form connections to the cathode. These ohmic contacts are formed by etching holes down through the N- layer 152 shown in Figure 6(D) to the level of the N+ buried layer 154 of the active region 146. These holes through the N- layer are aligned under two projecting fingers of Schottky metal 156 and 158 which form the cathode terminals. The outlines of these holes 148 and 150 are shown in dashed lines in Figure 6(C) under the projecting fingers 156 and 158. The ohmic contact is comprised of a structure consisting of 108 angstroms of germanium, 102 angstroms of gold, 63 angstroms of germanium, 236 angstroms of gold, 100 angstroms of nickel and 6000 angstroms of gold followed by a high temperature 450° C annealing step to form an alloy. The Schottky diode anode contacts are comprised of a three layer structure including titanium, platinum and gold formed in direct contact with the substrate. The projecting fingers 156 and 158 form the legs of a U-shaped island of Schottky metal best seen in Figure 6(C) at 160. This U-shaped island of Schottky metal is connected to the top plate 116 of the capacitor C1 by an air bridge 162 best seen in Figure 6(B). This air bridge is a bridge of conductive metal which joins the U-shaped island of Schottky metal shown at 160 in Figure 6(C) to the plated metal 116 of the top plate of capacitor C1. Capacitor C1, as best seen in Figure 6(B), is comprised of a top plate 18 of plated gold separated by a layer of nitride 164 from the bottom plate of the capacitor. The bottom plate of the capacitor is the layer of Schottky metal used to form the various components of the diodes and the ground plane 84.

The structure of the diode D2 on the left side of the center conductor 80 of the RF signal coplanar waveguide is similar to the structure of D1 except that a T-shaped island of Schottky metal shown at 168 is used to form the anode Schottky contact 140. This T-shaped section 168 is connected by an air bridge 170 to the top plate 118 of capacitor C2. This top plate is separated by the nitride layer 164 from the bottom plate of the capacitor comprising the Schottky metal layer 82.

All areas of the substrate shown in Figure 6(B) except the diode junction areas and the buried resistor 126 are proton implanted and semiinsulating.

The resistor R1 shown in Figure 1 is best seen in cross-section in Figure 6(B). An air bridge 170 couples the top layer 116 of the capacitor C1 to an island 172 of Schottky metal. This island 172 is formed over a ohmic contact hole which has been etched through the N-layer 174 to the N⁺ layer below. In Figure 6(B) only the resistor segment 126 is visible. The Schottky metal 172 contacts a gold-germanium alloy in contact with the N+ layer 126 to form an ohmic contact. A similar structure exists on the other side of the RF signal coplanar waveguide making contact between the top plate of the capacitor C2 and the resistor segment 124.

The method for forming air bridges is well known in the art of gallium arsenide processing but will be summarized here for completeness. A complete description of the process for fabricating the structure of the preferred embodiment is appended hereto as Appendix A. The first step in forming an air bridge between two metal patterns to be connected is to deposit the metal and pattern it to form the two nodes to be connected. Following this, a first layer of photoresist is deposited to coat the entire wafer. Thereafter the photoresist is developed in the area where the bridge is to be formed so as to leave contact holes to the metal surfaces to be electrically connected. Metal evaporation follows with an evaporation of 100 angstroms of titanium, 2000 angstroms of gold and another 300 angstroms of titanium being typical. This evaporated metal covers not only the exposed surface of the metal nodes to be connected but also the exposed surfaces of the photoresist. Next, a second layer of photoresist is deposited and developed to open a hole in the second layer of photoresist in the area where the air bridge is to be formed. The developing step for the second layer of photoresist includes formation of a contact hole to the evaporated metal layer for use in making contact for electroplating of a later defined gold layer. In the locations where the air bridge is to be formed, the top titanium is etched away to expose the underlying 2000 angstrom layer of gold. Then two microns of gold are electroplated onto the wafer by making electrical contact to the evaporated metal layer. After electroplating the gold, the top layer of photoresist is dissolved by spraying the wafer with acetone. This leaves the evaporated layers of titanium, gold and titanium in the areas outside the area of the bridge exposed. These three layers of evaporated metal outside the bridge are then etched away in a conventional manner. Finally, the wafer is dipped in acetone to dissolve the remaining layer of photoresist to leave the air

bridge standing between the two nodes to be connected.

Referring to Figure 7, there is shown in plan view a layout of the sampling diode portion of the preferred embodiment of the invention to show more detail regarding the interconnection of the various structural components. In Figure 7, structures which coincide with structures detailed on Figures 5 and 6, share the same reference numerals. The rectangular boxes inside the air bridge structures represent the metallic posts which support the air bridge. Rectangular boxes with Xs inside represent ohmic contacts to the underlying N+ layer. The multiplicity of air bridges across the gaps between ground plane conductors are used to maintain the separate segments of ground plane conductor at equal potentials so as to suppress even or slot line mode propagation. Because the mode of propagation for the sample pulses along the coplanar waveguide including center conductor 102 is even whereas the mode of propagation along the slot line portion of the RF signal coplanar waveguide is odd, there is little coupling between the RF signal coplanar waveguide and the coplanar waveguide carrying the sample pulses. Each coplanar waveguide has two propagation modes, CPW and slot-line. The odd mode, here called the CPW or coplanar waveguide mode, has electric field lines which point away from the center conductor across the gaps and toward the ground plane conductors. The even mode, here referred to as the slot line mode, has electric field lines which point in the same direction across the gaps between each ground plane and the center conductor. As long as the loading on the RF signal coplanar waveguide is symmetric about the center conductor, the slot line mode will not couple to the coplanar waveguide mode carrying the RF. It will be noted from Figure 7 that the sampling diodes and series capacitors connected across the slot are arranged to load the RF signal line symmetrically.

The intermediate pulses arriving in CPW mode from the nonlinear transmission line are coupled in slot line mode into the RF signal coplanar waveguide at point 90. After traveling for two picoseconds along the slot line in both directions, the intermediate pulses encounter an air bridge shorting together the two ground planes which form the slot line. Only one such air bridge is shown at 88 in Figure 7 with the air bridge to the left of the injection point 90 being out of view but shown at 86 in Figure 5. The air bridges short out the intermediate pulse waveform and brings the voltage back to 0 at the diodes after the four picosecond round trip time thereby shutting off the diodes. The resulting voltage waveform across the diodes appears as a differentiated version of the intermediate pulse.

The bandwidth of the sampler circuit is so

large, it can only be measured indirectly through a built-in TDR pulse generator shown at 138 in Figure 5. This built-in TDR pulse generator is identical to that used to generate the local oscillator intermediate pulses. The transition time at the output of the nonlinear transmission line 138 should be on the order of 2.8 picoseconds. The transition time measured by the sampling head is 4 picoseconds as shown in Figure 8. With a nonlinear transmission line having an 8.5 picosecond per millimeter reduction in fall time of a length sufficient to provide a falling edge of less than 2.5 picoseconds fall time with larger amplitude, it is possible with the sampler head design of Figure 7 to achieve sampling head bandwidth of 200-300 GHz. A larger intermediate pulse output amplitude will allow the differentiating slot line to be made narrower thereby eliminating the need for the hour glass shape of the RF sample coplanar waveguide. The hour glass shape is used in the embodiment shown in Figure 7 to emphasize the inductance by increasing path length so as to increase the amplitude of the sample pulses that turn on the diodes. Because the amplitude of the sample pulse is the derivative of the input voltage of the intermediate sample pulse times a constant equal to the inductance of the round trip path from the injection point to the air bridge and back again divided by the resistance of this path, increased inductance increases the voltage of the sample pulses across the diodes.

Improvement in the sampling bridge performance can also be made by using lower resistance diodes. In the embodiment shown in Figure 7, the junction area is 2×5 microns which results in a 12 femtofarad 0 bias capacitance. With suitable adjustments in geometry and doping, lower diode series resistance and possibly lower junction capacitance can be achieved.

The conversion efficiency of the sampling head design of Figures 5 through 7 when measured at 5 GHz and the intermediate frequency output port externally loaded by a 330 picofarad capacitance (cable capacitance of connections to chip) represented by capacitor C3 in Figure 1, and a 1 megohm parallel resistance, there was no voltage conversion loss within the accuracy of the measurement (0.5 dB). The power conversion loss was 43 dB which was also the approximate noise figure. This yields a minimum detectable signal of 90 nanovolts per square root Hertz. For an intermediate frequency bandwidth of 10 kHz, the minimum detectable voltage is 9 microvolts. The sampler was observed to be within 0.6 percent of linearity from -60 dBm to +3 dBm. The RF to IF isolation ("blow-by") was 55 dB, while local oscillator to IF isolation was 63 dB, and local oscillator to RF isolation ("kick-out") was 68 dB.

An ideal sampler would have perfect isolation

between all ports except at the intermediate frequency where a time scaled representation of the RF signal would appear with no voltage conversion loss in amplitude to any RF frequency. Further, the local oscillator and RF ports of an ideal sampler would be perfectly matched at all frequencies. When parasitics are accounted for in the sampler model, however, it is possible for the RF to couple directly or "blow-by" to the intermediate frequency port through diode capacitance and reverse leakage. Loss of isolation between the local oscillator and RF ports can occur if the bridge is not perfectly balanced or if the intermediate frequency drive is not balanced. Such imbalance can result in "kick-out" of the local oscillator pulse onto the RF line. Imbalance also causes a DC offset in the intermediate frequency voltage proportional to the local oscillator amplitude. These considerations must be taken into account when designing a layout for a structure according to the teaching of the invention.

Other layouts are possible besides structure illustrated in Figures 5 through 7. For example, a series capacitor arrangement could be used to differentiate the intermediate pulses, however, the layout shown in Figure 7 is more convenient since the parasitic inductance of the slot line differentiator is used to form the differentiating circuit.

Although the fabrication of the device is completely specified in Appendix A, a short summary of the fabrication is given here for completeness. Schottky diodes are formed on gallium arsenide molecular beam epitaxy material with a 0.6 micrometer N^- active layer with 3×10^{16} per cubic centimeter doping. A buried 0.8 micrometer N^+ layer with 3×10^{18} per cubic centimeter doping provides both the diode cathode connection and, on the nonlinear line, a resistive connection between the two coplanar waveguide ground planes, suppressing propagation of the slot line mode. Ohmic contacts having 0.02 ohms-millimeter resistivity are formed by a 0.75 micrometer recess edge, self-aligned gold/germanium/nickel/gold lift-off, and a 450°C alloy. Proton implantation using both 110 keV implant at a dose of 7×10^{14} per square centimeter and a 190 keV implant at a dose of 1×10^{15} per square centimeter. This proton implant damages the substrates sufficiently to provide greater than 40 megaohm per square isolation. During implantation, a 1.6 micrometer gold mask on top of a 1.4 micrometer polyimide layer protects the ohmic contacts on the diode active region. The interconnections are formed with 0.1 micrometer titanium/0.75 micrometer platinum/1.4 micrometer gold lift-off. Schottky diodes are formed in regions where the center conductor overlaps unimplanted N^- material.

In addition to millimeter wave Schottky diodes,

fabrication of this high speed circuit requires high capacitance per unit area capacitors and low capacitance air bridge crossovers. High capacitance per unit area is needed for capacitor C1 and C2 to allow reasonably high coupling capacitance diodes while maintaining a high capacitor self-resonance frequency. The capacitor resonates when it is one quarter wave length long. To set the self-resonant frequency to ten times the highest frequency of interest (10 x 100 GHz), for a 20 micrometer wide, 500 femtofarad capacitor with a silicon nitride dielectric, the dielectric thickness is must be 700 angstroms. A value of 1,000 angstroms was chosen for the dielectric thickness since nitride thinner than this can have an unacceptably high density of pin holes. 1,000 angstroms of nitride puts the resonant frequency at approximately 700 GHz for this structure.

Silicon nitride was chosen as the capacitor dielectric not only because of its high relative permittivity of 7.3 necessitated by the resonant frequency requirement discussed above, but also because of its excellent properties as a diffusion barrier and scratch protector. These are the same reasons that silicon nitride is the most widely used dielectric by microwave monolithic integrated circuit foundries. Choosing this dielectric in conformance with the existing industry standards also makes the sampling head circuit more practicable from the standpoint of manufacturability.

The capacitors are fabricated by depositing 1000 angstroms of 250°C PECVD silicon nitride over the entire wafer and reactive ion etching holes, in a C_2F_6 plasma, where contact is to be made to underlying metal. The bottom plate of the capacitor is the Schottky metal while the top plate is 2 micrometers of plated gold. An air bridge, which is plated at the same time as the capacitor, is used to make connection to the top plate.

The last element required for millimeter wave circuits of reasonable complexity is the air bridge. The air bridge, which is a cross-over with no supporting dielectric, can be made to clear the metal that is crossing over by 1.5 micrometers. This large gap, in addition to the unity dielectric constant of air, gives the air bridge cross-over extremely low capacitive coupling to the metallization below.

The air bridges are fabricated by the process summarized earlier herein and detailed in Appendix A.

Important features of the sampler design layout are: (1) monolithic integration with processing on one side of the wafer only; (2) fifty ohm input match at the RF port; (3) no degradation in RF signal as it propagates through the sampling structure; (4) sufficient bandwidth in the local oscillator connection for the ultra short sampling pulse; (5) a reasonable match on the local oscillator port; (6) a

balanced drive on the local oscillator port; and (7) an unbalanced drive on the RF port. The first requirement is the most demanding since it prohibits all previous sampling head designs. The structure detailed in Figures 5 through 7 to fulfill this requirement essentially consist of two intersecting coplanar transmission lines, one of which carries the local oscillator sawtooth waveform and the other which carries the RF signal to be sampled.

The slot line differentiator also provides a naturally balanced local oscillator drive. That is, the current in the center conductor of the local oscillator coplanar waveguide is equal and opposite to the current in the outer conductor. When this current is applied to the slot line mode of the RF signal coplanar waveguide, no current is induced on the center conductor of the RF signal line. Since no current is induced on the center conductor of the RF signal line, the potential of this conductor is determined by the RF circuit and not by the local oscillator.

When the intermediate pulses from the nonlinear transmission line are applied to the RF slot line, the initial impedance is that of the RF slot line in parallel with the sampling diodes, all in series with the 50 ohm local oscillator coplanar waveguide terminating resistance 110. To get the majority of the RF voltage to develop across the diodes instead of the terminating resistor 110, the RF slot line impedance must be as large as possible. To achieve the high impedance slot line segments, the RF ground planes must be separated by a significant fraction of the substrate thickness. To maintain the RF coplanar waveguide impedance at 50 ohms, the RF center conductor must also be made larger to keep the same center conductor to slot width ratio. This is another reason for the hour glass configuration of the center conductors 80 and the ground planes 82 and 84 shown in Figure 5. Scale modeling of the invention showed that a slot width on the RF slot line which is $3/8$ of the substrate thickness yields a slot line impedance of 78 ohms. Microwave simulations on SPICE indicate that this would be large enough to permit sufficient voltage to develop across the diodes. The requirement of the high impedance slot line mode in addition to the necessity of keeping the diode sampling loop short, results in the hour glass shape of the RF coplanar waveguide and keeps the RF coplanar waveguide at a characteristic impedance of 50 ohms.

A fundamental difficulty in making a sampling head with a bandwidth of 100 GHz or greater is to lay out the circuit in such a way that parasitic elements are eliminated or incorporated into the design. Any element that cannot be treated as a distributed structure must be kept much less than a wave length long at 100 GHz. In gallium arsenide,

this means all lumped elements must be less than 100 micrometers in their longest dimension. This requirement is easily met by the 2×5 micrometer sampling diode junction areas. However, it is desirable that the entire local oscillator circuit loop meet the 100 micrometer design rule to minimize inductance in this critical path. To accomplish this, minimum design rules were used to pack the elements as close together as possible. The thick Schottky metal lift-off process described earlier allows two micrometer lines and three micrometer spaces. When packed together, the local oscillator loop including the local oscillator terminating resistor 110, the two sample capacitors and the two sampling diodes measured 104 micrometers in perimeter.

NONLINEAR TRANSMISSION LINE DETAILED DESCRIPTION

Referring to Figure 17 there is shown a schematic diagram of a nonlinear transmission line. This transmission line will change the shape of an input signal shown generally at 10 and applied to an input terminal 12 to the output signal shown at 14 appearing at an output terminal 16. In the process of propagating from the input terminal 12 to the output terminal 16, the fall time of the signal 10 is reduced from the time $T_{i,in}$ to the fall time of the output signal equal to $T_{i,out}$. The input signal 10 is supplied by a signal generator 18 through a source resistance 20. The output signal 14 is applied to a load resistance 22.

The nonlinear transmission line between input terminal 12 and output terminal 16 is comprised of a plurality of segments. Each segment is comprised of an inductor L and a capacitor C. In the preferred embodiment, the inductance is implemented through short sections of transmission line marked XX in Figure 20. These short sections of transmission line have a characteristic impedance Z_1 and have a length in units of time which is designated in the equations of Appendix B as the Greek letter tau. Each capacitor takes the form of a varactor diode junction in the preferred embodiment. The capacitor in each section couples the center conductor 24 of the transmission line to a ground plane shown generally at 26. Thus, the first section of the nonlinear transmission line of Figure 17 is comprised of the inductor 28 and the varactor diode 30 having its anode coupled to the conductor 24 and having its cathode coupled to the ground plane 26. The conductor 24 serves as the center conductor. The varactor diode 30 has a PN junction therein which has a transition capacitance. The transition capacitance results when the junction is reverse biased and a depletion region is formed as

will be explained in more detail below. The transition capacitance is actually the change in uncovered charges of the depletion region as the voltage changes, but for discussion purposes the reader can visualize the capacitor as having two movable, conductive plates. These two conductive "plates" are separated by the depletion region when the diode junction is reversed biased. For completeness here, the transition capacitance and depletion region will be explained briefly so that the non-linearity of the transmission line can be understood by the reader. To do this requires reference to a cross section of the diode region.

Referring to Figure 18 there is shown a cross section of the transmission line at a location which shows the construction of one of the varactor diodes according to one embodiment of the invention. Figure 18 will be explained in much greater detail below during the discussion of the features of the transmission line. For now, the reader's attention is directed to a Schottky contact (diode junction) 38, a depletion region 34 and a N^- doped epitaxial layer 36 and an N^+ doped epitaxial layer 44. These three components along with ohmic contacts 46 and 48 form a Schottky diode. The dotted line defining the bounds of the depletion region 34 represents the extent of the depletion region into the N^- epitaxial layer 36 at a particular voltage level of reverse-bias on the Schottky diode junction. This depletion region 34 represents a volume of uncovered, immobile charges bonded in the N^- epitaxial gallium arsenide crystal lattice caused by the reverse-bias voltage. That is, the reverse-bias voltage causes mobile majority carriers donated by the dopants in the N^- epitaxial layer 36 to move away from the junction 38. In N^- material, these majority carriers are free electrons that are loosely bound to the nuclei of the N-type impurity atoms which have been added to the crystal lattice. When these mobile carriers move away from their nuclei under the influence of the negative potential applied to the anode of the diode, they leave uncovered the nuclei of the dopant atoms. These dopant atoms have one more proton than electron because of the movement of the electrons away from the junction, and thus represent immobile positive charges making up the depletion region 34. The dimension x_d represents the depletion region width. This dimension increases with increased reverse-bias voltage. Schottky contact 38 is the anode of the diode, and the N^- epitaxial layer 36 is the cathode of the diode. When a negative voltage is applied to the anode relative to the cathode, the diode is reverse-biased and the depletion region 34 is formed. If the level of reverse-bias voltage is increased, the dimension x_d increases as more electrons are pushed away from the junction and more positive charges are uncovered. This process

of uncovering charges represents the process of changing charge storage as voltage changes, which is the essence of a capacitor. This increase in uncovered charge with increases in applied voltage may be considered to be a capacitive effect. This capacitance is the transition capacitance which will hereafter be denoted $C_t(v)$. The magnitude of the transition capacitance is equal to the change in charge within the depletion region divided by the change in voltage which caused that change in charge. This capacitance is variously referred to in the literature as the transition region, space charge region, barrier region or depletion region capacitance. Because the depth of the depletion region 34 increases as V becomes more negative, the transition capacitance decreases with more negative voltages V .

The amount of change in the dimension x_d with the change in reverse-bias voltage depends upon the doping of the N^- epitaxial layer 36. Lighter doping leads to greater changes in the width of the depletion region for a given change in the reverse-bias voltage.

Referring again to Figure 17, what this change in the transition capacitance means in terms of the operation of the nonlinear transmission line is as follows. As the input signal 10 propagates along the transmission line, the instantaneous voltage at the anode of each diode changes over time. The input signal is applied with such a polarity relative to ground, that all diodes are reverse-biased. As the reverse-bias voltage on each anode changes, so does the transition capacitance magnitude. There is a total capacitance per section of line which is the combination of a fixed capacitance from the interconnecting line sections XX in Figure 20 which is not voltage dependent and the transition capacitance which is voltage dependent. Thus, the total capacitance per section of line is voltage dependent.

Many characteristics of the transmission line depend upon the transmission line capacitance per section. Where the capacitance per section is voltage dependent, so are these parameters. For example, the characteristic impedance of the line, the group delay and the group velocity of the line are all voltage dependent.

Precisely speaking, the mathematical relationship between the characteristic impedance and the voltage-dependent total capacitance per section of the line (denoted $C_T(v)$) is given in Equation 1 of Appendix B. The relationship between the group delay and the voltage dependent total capacitance per section of line is given in Equation 5 of Appendix B. The other equations of Appendix B define various other relationships of interest in considering the characteristics of a nonlinear transmission line. Equation 4 of Appendix B defines the precise

mathematical relationship between the capacitance of a step junction diode and the voltage applied to that junction to reverse bias it. Equations 6 and 7 of Appendix B give the relationships between the periodic structure cutoff frequency w_{per} and the diode cutoff frequency w_{rc} and the voltage dependent capacitance per section, the line inductance per section and the series resistance of the diodes. Generally, the higher these cutoff frequencies are, the shorter the falltime which can be achieved at the output of the line.

It is the voltage dependence of the group velocity which results in compression of the fall time of electrical wave fronts as they propagate along such a nonlinear transmission line. This compression can be understood by reference to Figure 19. Figure 19 shows the input signal 40 labeled V_{in} in part A and the output voltage labeled V_{out} in part B. The fall time of the input signal is labeled $T_{f,in}$. The fall time of the output signal is labeled $T_{f,out}$. Note that the fall time of the output signal is substantially shorter than the fall time of the input signal because of the compression which occurred during propagation down the line. The reason for this compression is that the points on the input voltage waveform having more negative voltages travel at higher speeds and experience less delay in a nonlinear transmission line than points on the voltage waveform having more positive voltages. This is because of the voltage dependence of the line capacitance and the relationship between the line capacitance and the group delay. This phenomenon is symbolized in Figure 19a by the delay vector labeled T_H for the point 40 on the input voltage wave form being longer than the delay vector labeled T_L for the point 42 which is lower on the voltage waveform. Every point on the voltage waveform has a different speed of propagation, and hence a different delay through the line. Because the higher voltage points are traveling faster and have less delay than the lower voltage points, the "tops catch up with the bottoms" and the waveform changes shape and assumes the shape of the output waveform known at Figure 19b. The result is that the fall time is compressed as seen by the substantially shorter duration of $T_{f,out}$ in Figure 19b, compared to $T_{f,in}$ in Figure 19a. The reasons why higher voltage points have faster speeds of propagation are described in Appendix B and are well understood by those skilled in the art and no further details will be given here.

Referring to Figure 20 there is shown a plan view of the nonlinear transmission line according to the preferred embodiment of the invention. The structural details of the transmission line can best be understood by joint reference to Figures 2, 4, 5 and 6. Figure 18 shows a cross-section of one of the diodes in the transmission line taken at section

line 2-2' in Figure 20 according to one process of fabricating the line. The transmission line is fabricated on a monolithic gallium arsenide substrate 42. This substrate has formed thereon an N^+ epitaxial layer 44 and an N^- epitaxial layer 36 formed on top of the epitaxial layer 44. In Figure 20, only a portion of these epitaxial layers is visible between the ground plane metal contacts 26 and the center metal contact 24. This epitaxial layer portion is labeled 36/44. The two parallel metal conductors 24 and 26 form the inductive portions of the transmission line. The center conductor 24 also forms the anode contact of the Schottky diodes. The ground plane contact 26 is also the cathode contact of the Schottky diodes. These cathode contacts are implemented with ohmic contacts to the N^+ epitaxial layer 44 as best shown in Figure 18.

The ohmic contacts 46 and 48 are formed by alloying a gold germanium mixture at high temperatures as is well known in the art. Any ohmic contact alloy will work to form the contacts 46 and 48, but it is preferred to use an alloy and a technique which will create the lowest possible contact resistance for reasons which will be explained more fully below. In the preferred embodiment, the ohmic contacts 46 and 48 are formed by heating a mixture of 8% gold and 12% germanium so as to cause the germanium to diffuse into the N^+ epitaxial layer 44 to form a low resistance contact. The ground plane metal contact 26 and the center anode contact 24 are each comprised of gold. Two diffusion barrier layers 50 and 52 in the ohmic contact structure prevent the gold from the ground plane conductor 26 from diffusing into the ohmic contact regions 46 and 48 or the N^+ epitaxial layer below it. This prevents spiking of gold through the N^+ epitaxial layer 44 to the substrate 42. Preferably, the metal/dopant alloy chosen for the ohmic contacts will have as low a melting point as possible. Other nonalloyed contact structures may also be used if spiking of the gold through to the substrate 42 can be prevented. It is important, however, for the contact structure chosen to have a low series resistance so as to maintain the diode cutoff frequency as high as possible.

The diode-anode contacts are formed by the gold layer 24 on top of a platinum diffusion barrier 54. The platinum diffusion barrier separates the gold layer 24 from the Schottky contact metal 56 and prevents the gold layer 24 from spiking through the Schottky junction to the buried layer 44 and shorting the diode. The Schottky contact metal layer 56 is titanium in the preferred embodiment. However, many other metals may be used for the Schottky contact metal layer 56. Basically, any metal that will form a Schottky diode may be used. Such metals include aluminum, molybdenum, chromium and alloys such as molybdenum/aluminum

and titanium/tungsten. The desired qualities for the metal layer 56 are that it exhibit good adhesion to the gallium arsenide substrate and that the diffusion of the metal into the gallium arsenide be low during high temperatures of operation or during subsequent processing steps. It is also desirable that the material chosen for metal 56 be stable in the sense that it should not change the leakage current through the diode with aging, changing temperature and so on. For further information, see page 271 of the text on gallium arsenide processing incorporated by reference herein.

The liftoff process for forming the diode anode contact 56/54/24 is well known in the art of semiconductor processing and is described in more detail at page 145 in "Gallium Arsenide Processing Techniques" incorporated by reference herein. For completeness here, a short summary of the process will be given. In the area where metal is to be placed on the substrate, a layer of photoresist which has been spun onto the wafer is exposed to light through a mask. All other areas are shaded by the mask. The layer of photoresist is then hardened at the surface by a chlorobenzene soak before being developed. This renders the surface farthest away from the gallium arsenide harder than the regions closer to the substrate. The layer of photoresist is then developed. Because the developer carries away material closer to the substrate faster than the harder material farther away from the substrate, the area of photoresist exposed to the light is carried away and forms a hole with inwardly tapered edges. Then the desired metal is evaporated onto the surface of the substrate in the hole in the photoresist and onto the surface of the photoresist itself. Thereafter, the photoresist is dissolved thereby carrying away the metal on top of the photoresist and leaving the metal in the hole in the photoresist layer attached to the substrate there. This process is used to form the diode anode contact, the final interconnect metallization, and the ohmic contacts. It is also used to form the implant mask except that a layer of polyimide is placed under the layer of photoresist such that the metal in the hole in the photoresist is formed on top of a layer of polyimide. After the metal liftoff, the metal in the hole lies on top of a layer of polyimide covering the whole wafer. The wafer is then immersed in commercially available polyimide solvent to dissolve all the polyimide except that portion of the layer under the metal. The resulting metal/polyimide sandwich acts as an implant mask during the proton isolation implant.

Other gate technologies could also be used to form the Schottky diode anode contact. Some of these other gate technologies may have reduced reliability over time when subjected to high temperatures.

The doping of the N^- epitaxial layer 36 is 3×10^{16} N_D atoms/cm³. The doping of the N^+ epitaxial layer in the preferred embodiment is 3×10^{18} N_D atoms/cm³.

The Schottky diodes are formed by isolating the epitaxial layers so that there are periodically spaced, isolated islands of epitaxial layers 36 and 44 which have mobile charge carriers therein. An implant is used at all other areas to cause crystal damage in the epitaxial layers 36 and 44 to immobilize the charge carriers, thereby converting the epitaxial layers in these implanted regions back to what is essentially intrinsic, high resistivity gallium arsenide. This crystal damage region is shown as the speckled pattern in the epitaxial layers 36 and 44 at 54 and 56 in Figure 18. In Figure 21 viewing above the plane of the nonlinear transmission line, the crystal damage region includes the entire area of the devices except for the masked regions 62 in which the diodes are formed. Outside the masked (unimplanted) regions 62, the implantation converts the N^- and N^+ layers into semi-insulating material, thus restricting the Schottky contact area 38 to within the unimplanted region 62. These isolation regions restrict the current path to the dotted lines shown passing through the N^- epitaxial layer 36 and the N^+ epitaxial layer 44 from the depletion region to the ohmic contacts. These current paths are designated 58 and 60 in Figure 18.

A plan view of the boundary of the isolation island for each Schottky diode is illustrated in Figure 21. In Figure 21, the dashed lines represent the outline of the metal contacts 24 and 26, while the solid line 62 represents the boundary of the isolation implant. All area within the solid line 62 is not implanted. Thus, the charge carriers in the epitaxial layers 36 and 44 within this perimeter will be free to move.

Referring to Figure 22 there is shown a plan view of the area of a typical diode. The dashed lines 64 and 66 define the perimeters of the ohmic contacts 46 and 48. The region 38 defined by the intersection of the areas of the central metal contact 24 and the isolation island 62 defines the junction area of the Schottky diode.

The dimension P in Figure 20 defines the pitch or periodicity of the diodes. In the preferred embodiment, the pitch is 160 microns. Ten micron design rules are used in the preferred embodiment, which means that the junction area 38 in Figure 22 of the diode is 10 microns x 10 microns. This also means that the space between the center conductor 24 and the ground plane conductors 26 is also 10 microns. Smaller junction areas and closer spacing will improve the performance of the device for reasons which will be explained in more detail below.

The minimum compressed fall time $T_{f,min}$ is set

predominantly by the periodic line cutoff frequency and the varactor diode RC cutoff frequency ω_{rc} . The expressions for these two cutoff frequencies are given by Equations 6 and 7 of Appendix C. With monolithic fabrication of the transmission line on gallium arsenide substrates, these two cutoff frequencies can be on the order of 0.1 -1 terahertz. This permits obtaining compressed fall times on the order of 5 - 10 picoseconds with 10 micron design rules. In the preferred embodiment, the integrated nonlinear transmission line incorporates 42 diodes. Each of these diodes has a junction potential ϕ of approximately 0.8 volts and C_{jo} of approximately 50 femtofarads at 160 micron spacing ($\tau = 1.4$ picoseconds) along a 90 ohm coplanar waveguide transmission line. This results in a 140 gigahertz periodic line cutoff frequency. By calculation, the characteristic impedance $Z_0(v)$ varies from 44 - 55 ohms, and the group delay $T(v)$ changes by 25 picoseconds as the line voltage varies from 0 to -2 volts.

In Figure 18, the N^- epitaxial layer 36 is 0.6 microns thick in the Z direction. The N^+ epitaxial layer 44 is 0.8 microns thick in the Z direction in the preferred embodiment. The current in the diodes travels from the anodes to the cathodes along the paths 58 and 60 in Figure 18. There is a series resistance associated with the current paths 58 and 60 which is the series resistance of the diode which limits the diode cutoff frequency ω_{rc} . This series resistance can be divided into three components.

The first component is the resistance of the current path in the portion of the N^- epitaxial layer 36 from the bottom of the depletion region 34 to the junction with the N^+ epitaxial layer 44. This component of resistance accounts for approximately 20% of the total series resistance, and varies as the depth of the depletion region 34 varies with voltage. The second component of the resistance is the component attributed to the flow of the current through the N^+ epitaxial layer 44 to the positions of the ohmic contacts 46 and 48. This component accounts for approximately 60% of the total series resistance. The remaining 20% of the total series resistance is attributed to the resistance of the ohmic contacts 46 and 48. Obviously, closer spacing of the ground plane contacts 26 to the center contacts 24 will decrease the total path length and the total series resistance. Also, improvement of the ohmic contacts series resistance will raise the diode cutoff frequency.

The N^+ epitaxial layer 44 also provides a resistive connection between the two coplanar waveguide ground planes labeled as metallic contacts 26 in Figure 18. This resistive connection suppresses propagation of an undesired unbalanced "slot-line" mode on the transmission line.

Fabrication of the device of Figure 18 is performed in the following manner. Fabrication starts with an undoped gallium arsenide substrate which has a sufficient length to get a sufficient number of sections of the transmission line to achieve the desired degree of compression. In the preferred embodiment, 42 diodes are used at 160 micron center to center spacing. The minimum number of diodes required in the line is approximately 20% larger than the quantity equal to the falltime of the input signal ($T_{i,m}$) divided by the difference in delay between the highest voltage point and the lowest voltage point of the waveform. This delay is given by Equation 5 of Appendix C. The factor of 20% is necessary because compression to the final, shortest falltime is approached asymptotically.

The first actual process step is to grow the two epitaxial layers 36 and 44. In the preferred embodiment, these layers are grown by molecular beam epitaxy to the thicknesses cited above. Any other epitaxial method will also work to grow these layers. For example, liquid or vapor phase epitaxy will work as well as MOCVD which stands for metal organic chemical vapor deposition. Methods of performing this process and other process steps described herein are described in more detail in "Gallium Arsenide Processing Techniques" by Ralph Williams, ISBN 0-89006-152-1 (Artech House, Inc. 1984) which is hereby incorporated by reference.

The epitaxial layers are doped as they are formed to have uniform doping profiles with the doping levels given herein. It is not believed that diffusion can be used to dope the epitaxial layers since it would not be possible to dope the epitaxial layer 44 heavily without leaving a doping level in the epitaxial layer 36 which is too high.

Next, the two ohmic contacts 46 and 48 are formed having 0.06 ohms/mm resistivity. These contacts are formed using a 0.75 μ m recessed etch, a self-aligned (88% gold-12% germanium)-/nickel/gold liftoff technique, and a 450°C alloy or a 12 second rapid thermal anneal. The rapid thermal anneal process is preferred since lower contact resistance can be achieved.

Figure 23 shows the state of the wafer after formation of the two epitaxial layers 36 and 44 and after deposition of the ohmic contact metals and just prior to the liftoff. The layer of photoresist 68 represents the configuration of the first mask level. The contact holes 70 and 72 are etched using the photoresist layer 68 as the etch mask. This etch is performed using a wet chemical etch because of the 10 micron design rules. If 2 micron design rules are used, in alternative embodiments, the etch step to form the contact hole 70 and 72 may be performed using a plasma etch. After the contact holes are etched through the N^- epitaxial layer

36, a conventional metal evaporation step is performed. This metal evaporation step uses the photoresist layer 68 to protect all layers of the N⁻ epitaxial layer 36 except the areas where the contact holes 70 and 72 are formed. To do this, the wafer is placed in a chamber which is pumped down to a high vacuum level. Then a high energy electron beam is directed at a crucible filled with a gold-germanium mixture comprised of the desired alloy. The electron beam evaporates portions of this mixture in the center of the crucible causing gold and germanium atoms in the prescribed proportion to be deposited as the first layer of the ohmic contacts labeled 46 and 48 in Figure 23 and as the layer 74 on top of the photoresist layer 68. After this layer has been deposited, the gold-germanium target crucible is rotated out of the path of the electron beam and a crucible containing nickel is rotated into the path of the beam. The high energy electron beam then evaporates portions of the nickel in the target crucible causing nickel atoms to be deposited on top of the previously deposited gold-germanium layer. This nickel layer is labeled 50 and 52 in the positions of the ohmic contacts and 76 on top of the layer 74.

After these two metal layers are deposited, the photoresist layer 68 is dissolved in a chemical bath thereby removing the metal layer 74 and 76. In some embodiments, a further layer of gold (not shown) is evaporated on top of the nickel layers 50 and 52 prior to removal of the photoresist layer 68. In these embodiments, the photoresist layer 68 is removed after this gold layer is deposited. The entire structure then is subjected to a 450°C alloy process in a diffusion furnace for 30 seconds or for 12 seconds in a rapid thermal anneal device. During this high temperature step, germanium atoms in the metal layers 46 and 48 diffuse into the N⁺ epitaxial layer 44, thereby forming a low resistance ohmic contact. During this high temperature step, the nickel layers 50 and 52 act as diffusion barriers to prevent gold deposited on top of the nickel from diffusing into the gold germanium layers 46 and 48. This also prevents the gold from diffusing into the epitaxial layer 44 and "spiking" through to the gallium arsenide substrate 42.

The next step is a proton implantation for the purpose of defining the isolation islands in which the Schottky diodes will be formed. Figure 24 shows the proton implantation step and the configuration of the gold 77/polyimide 78 implantation mask which defines the boundaries of the isolation island. The implantation mask 77/78 has a configuration from the plan view, i.e., looking down the Z axis, as shown in Figure 21. The purpose of the isolation implantation has been previously described. Only the portions of the epitaxial layers 36 and 44 lying underneath the implantation mask

77/78 will be able to conduct current freely after the implantation step has been performed. In the preferred embodiment, the implantation is done using protons since protons are relatively easy to implant to the necessary depth into gallium-arsenide at energy levels around 190 KEV. However, some equipment having greater acceleration energies is available to implant other types of ions such as oxygen or boron to the necessary depth. Any such implantation which causes the above described crystal damage result will suffice for purposes of practicing the invention. In the preferred embodiment, the proton implantation is done in two steps. The first step is an implant at 190 KEV with a dosage level of 6×10^{14} /sq. cm. The second step is a 160 KEV implant with a dosage level of 1.5×10^{14} /sq. cm. These implants provide a greater than 40 megohm/sq. isolation characteristic. The isolation mask 77/78 is comprised of 1.6 micrometers of gold shown at 77 and 1.4 micrometers of polyimide 78 overlying the ohmic contacts and the region 62 which will become the diode-active region.

The final process step is to perform a third mask level photolithography step to define by liftoff techniques the locations of the Schottky anode contacts 24 in Figure 18 and the configuration of the ground plane metal contacts 26. After the resulting photoresist layer is developed, metal evaporation is used to deposit 0.1 microns of titanium as shown at 56 in Figure 18. After the titanium is deposited, the titanium crucible is rotated out of the way and a platinum crucible is rotated into the target position. The high energy electron beam then is applied to evaporate a portion of the platinum in the center of the crucible to deposit a 0.1 micron platinum diffusion barrier shown at 54 in Figure 18. Finally, the platinum crucible is rotated out of the way and a gold target crucible is rotated into the target position. The third evaporation step is then performed to deposit a 1.4 micron thick (Z direction) gold contact 24 and to form the gold ground plane contacts 26 and transmission line conductors 24. In some embodiments, the ground plane contacts 26 and transmission line conductors 24 may be formed separately with a fourth masking level. Schottky diodes are formed in a 10 micron by 10 micron region underlying the titanium layer 56 in each isolation island by the self aligned intersection of the titanium metal deposition and the isolation island. This completes the fabrication of the device.

With a nonlinear transmission line of the structure of Figures 2 and 4, it is possible to configure the dimensions of the structure to obtain compressed fall times which are short enough to generate gate impulses of approximately 5 picosecond duration or better. Such a gate impulse can be

obtained by differentiating the output step transition after compression in a nonlinear transmission line of the structure of Figures 2 and 4. The band width of diode sampling bridges used in sampling oscilloscopes and network analyzers is primarily limited by the duration of the pulse gating the diode. With gating pulses having approximately 5 picoseconds duration, the bandwidth of 2 diode sampling bridges for sampling oscilloscopes could be extended from the current 20 gigahertz level to 100 gigahertz.

One of the factors which limits the shortest falltimes which are available from a nonlinear transmission line of the structure shown in Figures 2 and 4 is the cutoff frequency for the Schottky varactor diodes. This cutoff frequency, is defined by Equation 7 of Appendix C. Another factor which limits the amount of compression is the cutoff frequency of the periodic structure. This cutoff frequency is defined by Equation 6 of Appendix C. With the configuration of the nonlinear transmission line of Figures 2 and 4 and with some scaling of the structural dimensions using more stringent design rules, it is possible to obtain step functions with the falltimes of approximately 4 picoseconds. This is a factor of 6 improvement over the rise times which can be currently attained by electrical means. With further improvements in the process and with tighter design rules, it is possible to obtain subpicosecond rise times.

What is the relationship between the physical dimensions of the structure shown in Figures 2 and 4 to the amount of compression which can be obtained? As a step input signal $V_{in}(t)$ with initial voltage v_i , final voltage v_f , and fall time $T_{f,in}$, propagates along the line, the fall time will at first decrease linearly with distance. As the pulse fall time decreases, dispersion arising from the structure's cutoff frequency, w_c , competes with the compression arising from the voltage-dependent propagation velocity. A final limited fall time $T_{f,min}$, on the order of, but longer than $2.2/w_c$, is reached at which the edge compression per section due to line nonlinearity is equal to the edge broadening per section due to line dispersion. The output fall time is given by Equation 8 of Appendix C. $T_{f,min}$ in Equation 8 varies inversely with both the diode cutoff frequency w_{rc} given by Equation 7 and the periodic cutoff frequency w_{per} given by Equation 6. Exact calculation of $T_{f,min}$ requires computer simulation.

Line periodicity of the diode structure introduces a cutoff frequency w_{per} which is given by the implicit relationship of Equation 9 of Appendix B which is simplified to Equation 6 of Appendix B. The term C_{ls} in Equation 9 is the varactor's large signal capacitance and is defined by Equation 10 of Appendix B.

For input signals $v_{in}(t)$ such that at all points on

the line the propagating wave is of sufficiently long rise time, the output of the transmission line is given by Equation 11 of Appendix B. This equation shows that the compression occurs because of the voltage dependence of the propagation velocity signal along the line as shown by the relationship between equations 11 and 5.

The performance of the line can be improved by increasing the periodic cutoff frequency w_{per} . This can be done by decreasing the diode spacing (in units of τ). However, decreasing τ (decreasing pitch) will also decrease the small signal characteristic impedance given by Equation 1 of Appendix B and will also decrease the large signal characteristic impedance given by Equation 12 of Appendix B because of the decrease in inductance per section (given by Equation 1 of Appendix B) where the characteristic impedance of the line is defined by Equation 12 of Appendix B. This is an undesirable result for the power transfer efficiency reasons noted above. Therefore, the large signal characteristic impedance Z_{ls} given by Equation 12 in Appendix B will be constrained to approximately 50 ohms for purposes of practicing the invention. Other embodiments according to the teachings of the invention may use different characteristic impedances for specific applications. However, the preferred embodiment will have a characteristic impedance of approximately 50 ohms. Accordingly, to satisfy this constraint while decreasing the diode spacing τ , the large signal varactor capacitance C_{ls} must also be scaled in proportion with the scaling of L , the transmission line inductance per section. In such a case, the periodic cutoff frequency w_{per} is limited by lithographic constraints on the minimum junction area for the varactor.

The varactor series resistance r_s introduces a varactor cutoff frequency of w_{rc} . If this cutoff frequency is much less than the periodic cutoff frequency w_{per} , this varactor cutoff frequency limits the compressed rise time to approximately $2.2 r_s C_{ls}$. This time constant is the fundamental limitation to the compressed fall time, assuming elimination of the periodic line cutoff frequency w_{per} . Of course, neither cutoff frequency can be eliminated in reality so both effects must be taken into account.

The total circuit area of the structure shown in Figures 2 and 4 with 10 micron design rules and 160 micron diode spacing along a 90 ohm coplanar wave guide transmission line is approximately 8 mm by 0.3 mm. With a periodic line cutoff frequency of approximately 140 gigahertz, the minimum compressed fall time of 4 pico seconds can be obtained if the diode resistance is zero. With 10 ohm diode resistance, minimum compressed falltimes of 7.5 picoseconds can be obtained.

To generate subpicosecond pulses with a non-linear transmission line, both the line periodicity cutoff frequency w_{per} and the varactor cutoff frequency w_{rc} must be increased. Because of the constraints on line impedance in the preferred embodiment of 50 ohms or thereabouts, diode spacing (L) must scale with diode junction area ($C_{j(v)}$). To decrease the diode capacitance and increase w_{per} , either the device-active layer doping must be decreased below 3×10^{16} atoms/cm³ or the junction area must be decreased below the 10 micron by 10 micron area described herein. Because of degraded diode cutoff frequency and because of rapid increases in the depletion layer width, x_d in Figure 18, with decreases in the doping of the N⁻ epitaxial layer 36 requiring much thicker N-layers to avoid possible punch through, capacitance reduction through reduction in the junction area is the more desirable of the two approaches.

Increased varactor cutoff frequency w_{rc} can be achieved by decreasing diode series resistance r_s . This can be achieved by reducing the spacing of the ohmic and Schottky contacts. In Figure 18, decreased contact spacing would translate to smaller dimensions A_1 and A_2 . This would decrease the length of the current paths 58 and 60 thereby reducing the series resistance. Further improvements in the series resistance can be made by selecting the ohmic contact material in process so as to minimize the series resistance presented by the ohmic contacts 46 and 48, by heavier doping of the N⁺ epitaxial layer 44, and by optimization of the thickness of the N⁻ epitaxial layer 36 to the maximum possible depletion layer width x_d . That is, the thickness of the epitaxial layer 36 should be made as close as possible to the maximum penetration of the depletion layer 34 into the N⁻ epitaxial layer 36. This minimizes the current path segment from the edge of the depletion layer 34 to the junction between the epitaxial layer 36 and the epitaxial layer 44.

Figure 17 is a graph of the compression of a 500 picosecond input fall time to a 100 picosecond output fall time on a scale model of the invention which was constructed with very large geometries.

Figures 10 and 11 show an alternative embodiment of the invention. Figure 170 is a cross-section through one of the diodes of a nonlinear transmission line where the N⁻ epitaxial layer has been etched away at all locations except the area under the Schottky diode anode contact.

Figure 171 shows a cross-section through the transmission line at a location other than the location of a diode active area.

Figure 172 schematically shows another alternative structure according to the teachings of the invention. In this structure, the diode junction areas are decreased at each diode location from the

input of the line to the output. Further, the spacing between the diodes is scaled in proportion to the decrease in the junction area such that the characteristic impedance of the line remains approximately 50 ohms. The purpose of such an embodiment is to achieve improved performance. This improved performance results from the recognition that as the signal propagates down the line, its fall time is compressed and the high frequency components in the spectrum of the signal therefore increase. These high frequency components change the impedances presented by the capacitances of the diodes and the inductance of the coplanar wave guide sections unless the size of the junction and the spacing between the junctions is altered. Figure 172 shows the junction areas and junction spacings from plan view only. All other details of the construction are as previously described. Another possible embodiment is to construct the transmission line in segments, each segment containing a plurality of diodes. In the first segment, the diodes will have a first junction area in a first spacing. In the second segment, the junctions will all be the same size but smaller than the size of junctions in the first section. Further, the spacing between the diodes in the second section will be closer in proportion to the decrease in the junction area so as to maintain the characteristic impedance of that section at approximately 50 ohms. This pattern of ever-decreasing junction area and spacing between the diodes in each section is repeated until the appropriate length for the transmission line is achieved. The first several sections are designed to maximize the change in delay with voltage, thus reducing the total number of diodes required for a given input falltime $T_{f, in}$. The later sections with smaller geometries have higher diode and periodic cutoff frequencies, and are optimized to obtain the shortest possible output falltimes.

Other possible structures which can be used to achieve compression according to the teachings of the invention are any capacitance which is voltage dependent. Thus, for example, regular PN diode junctions could be used as opposed to Schottky diodes to create the nonlinearity and voltage-dependent propagation velocity needed to achieve the compression. A cross-section of the diode portion of the transmission in such an embodiment is shown in Figure 173. In the diode structure of Figure 173, layer 80 is a gold diode contact. Layer 82 is an ohmic contact. Layer 84 is P type epitaxial gallium arsenide which is doped to give a minimum amount of series resistance in current flow through the P epitaxial layer 84, to the N⁻ epitaxial layer 86. The N⁻ epitaxial layer 86 is formed and doped in accordance with the description given above for the epitaxial layer 36. Finally, the N⁺ epitaxial buried layer 88 is formed and doped in accordance

with the description of the N^+ epitaxial layer 44 given above. In alternative embodiments, the P type epitaxial layer 84 could be doped P^- .

In yet another alternative embodiment, hyperabrupt Schottky contacts are used to fabricate a line which otherwise has the construction shown in either Figures 2 and 4 or Figures 10 and 11. Such a hyperabrupt junction is represented by Figure 174 where the increased density of the dot pattern near the surface of the N^- epitaxial layer represents a heavier doping there. A hyperabrupt Schottky contact requires that the N^- epitaxial layer have a nonuniform doping. Such an N^- layer is lightly doped at the N^-/N^+ epitaxial layer junction. This doping increases as one moves through the N^- epitaxial layer in the positive Z direction. Such a doping profile can be manufactured using molecular beam epitaxy, liquid phase epitaxy or MOCVD. It is also possible to form such a nonuniform doping profile using ion implantation. In such an embodiment, the N^-/N^+ epitaxial layers would be formed with molecular beam epitaxy and doped using an ion implantation. The doping profile is adjusted to make the capacitive changes linear for linear changes in the instantaneous line voltage applied to reverse bias the junction. In the preferred embodiment, the change in capacitance for a unit change in reverse bias voltage is nonlinear in that for higher levels of voltage, the unit change in applied reverse bias voltage produces less change in the capacitance than a unit change in voltage at a lower voltage causes. By adjusting the doping profile appropriately, the changes in capacitance for a given change in voltage can be made linear throughout the range of voltages of the input signal. The main reason for using hyperabrupt junctions is to get larger changes in capacitance per unit change in voltage. That is, with a hyperabrupt junction, the capacitance of the resulting junction varies more rapidly with voltage than the capacitance of a junction with uniform doping, producing a greater change in line delay with input voltage. For a given input signal falltime $T_{f,In}$, the required number of diodes and hence the required line length is decreased.

Another alternative embodiment according to the teachings of the invention is to reduce the size of the overall die using spiral inductor sections to replace the inductive transmission line sections marked XX in Figure 20. The spiral inductor sections are publicly known and exist on various devices manufactured by Pacific Monolithics of Sunnyvale, California.

Another alternative embodiment which could be used according to the teachings of the invention is in the form of a monolithic coplanar wave guide loaded periodically with the gate capacitances of a series of MESFET's. A cross-section through the

MESFET of such a device is shown in Figure 175. In such a device, layer 92 is the gate metal and layer 94 is N^- epitaxial gallium arsenide lying on top of a substrate of gallium arsenide (not shown). Layers 96 and 98 are N^+ epitaxial layers which make contact with source and drain metal contacts 100 and 102.

A detailed process schedule for the preferred embodiment of a process according to the teachings of the invention is given in Appendix C. The process schedule of Appendix C results in a structure as shown in Figure 176. The only difference between the structure of Figure 176 and that shown in Figure 18 is the existence of the additional layers of titanium 106 and platinum 108 above the ohmic contact metal. These additional layers do not affect the resistivity of the contacts substantially.

Alternative process technology can also be used to fabricate the device structures described above. Although in the preferred embodiment of the process according to the teachings of the invention, a standard $NH_4OH/H_2O_2/H_2O$ gallium arsenide wet etch is used to give good etch depth control needed for etching through the N^- layer to the buried N^+ layer for the ohmic contact and initial alignment marking etch, other etch processes may also be used. For example, dry etch or plasma etch processes may be used if sufficient depth control can be achieved to prevent etching through the N^+ epitaxial layer. Dry etches create surface states, but it is possible that these surface states can be etched away with a mild wet etch following the dry etch.

In the preferred embodiment, ohmic metallization is a typical germanium-nickel-gold eutectic mixture deposited by electron beam evaporation and alloyed in a rapid thermal annealer. The rapid thermal anneal process is faster, easier, cheaper and more reproducible than a conventional oven anneal process and is therefore preferred. Ohmic contacts of 0.06 ohms/mm resistivity have been achieved which is much lower than the typical values quoted for oven annealed contacts (typically 0.5 to 5 ohm-mm). Although this ohmic contact metallization is achieved using liftoff metallurgy (additive) it is also possible to perform this metallization as well as the other metallizations in the process using subtractive etching processes. Either wet etch or dry etch processes may be used for the subtractive etching. The liftoff technology avoids problems of semiconductor surface etching, and is therefore preferred.

The implant isolation masking is an important step. Since high energy, high dose proton implant masking is required, the preferred embodiment uses a 1.6 micron layer of gold on top of a polyimide layer. This layer is patterned using a

thick metal liftoff process. However, this implant mask could also be performed by subtractive processing using either wet or dry etches to define the implant mask. The liftoff process works quite well, and the metal thickness for the gold layer can even be increased to provide better implant masking. Better implant masking permits higher implant energies, which will result in a greater depth of penetration of the implant into the N^- layer 36 and the N^+ semiconductor layers. A thicker N^+ layer can then be used, reducing the diode series resistance, as is described subsequently. Thicker metal on the implant mask for subtractive processing means longer etch times and possibly lateral etch problems if wet etches or isotropic dry etches are used for subtractive processing. Therefore, liftoff processing is preferred.

Although the final level interconnect metallization requires very thick layers of gold, subtractive etch processing may also be used for this metallization as opposed to the thick metal liftoff process currently used in the preferred embodiment of the process. The thick metal of this metallization is necessary to achieve low line series resistance. This resistance is currently 12 ohms in the preferred embodiment.

As geometries are scaled down to achieve higher performance levels, self-alignment techniques for the fabrication will become more important. Currently, the Schottky diode junction area and the ohmic contacts are formed using self-aligned process steps. In alternative embodiments, the spacing between the central metal conductor 24 and the ground plane conductors 26 may also be performed using self-aligned processes.

Finally, in the preferred embodiment, the N^+ epitaxial layer 44 is formed at a thickness of 0.8 microns to keep the resistance of the current paths 58 and 60 in Figure 18 to a minimum. Thicker layers for this epitaxial layer 44 may be used to further lower their resistance. However, for areas outside the diode isolation island, isolation implantation must be performed. Where thicker layers of epitaxial material 44 are used, higher energies for these isolation implants will be necessary. Alternatively, some etch step may be used to remove the epitaxial layers at regions outside the isolation islands. Preferably, this etch step should be self-aligned so as to not destroy the ohmic contacts 46 and 48.

It is also possible to use self-aligned gate techniques to align the Schottky junction area between the ohmic contacts when the dimensions of the structure are scaled to very small geometries. One possibility is to use refractory metal gates in a T shape. The bottom of the T then serves as the Schottky contact while the top of the T serves as an etch mask to define the positions of the inner

edges of the contact windows for the ohmic contacts.

Although the invention has been described in terms of the preferred and alternative embodiments disclosed herein, those skilled in the art will envision other embodiments which may be used without departing from the teachings of the invention. All such embodiments are intended to be included within the scope of the claims appended hereto.

Claims

1. An integrated sample head, comprising:
a substrate of semiconductor material having one surface suitable for integration of circuitry thereon;
first means integrated on said one surface for receiving sample pulses having a first rise time and for reshaping said pulses into intermediate pulses having a second, substantially faster rise time;
differentiation means integrated on said one surface coupled to receive said intermediate pulses and differentiate them to generate sample pulses having a pulse width substantially equal to said second rise time;
RF waveguide means integrated on said one surface for receiving a high frequency, repetitive signal to be sampled and for guiding along said surface; and
sampling means integrated on said one surface and coupled to said RF waveguide means and coupled to receive said sample pulses, for generating an output voltage at the time of each sample pulse which is substantially equal to the amplitude of said signal to be sampled at the time of said sample pulse.
2. The apparatus of claim 1 wherein said substrate is gallium arsenide.
3. The apparatus of claim 2 wherein said first means comprises a nonlinear transmission line characterized by periodic loading by voltage dependent shunt capacitances.
4. The apparatus of claim 3 wherein said nonlinear transmission line is an integrated coplanar waveguide periodically loaded with Schottky diodes.
5. The apparatus of claim 3 wherein said differentiation means includes an integrated coplanar waveguide coupled to said nonlinear transmission line so as to excite slot line mode propagation.
6. The apparatus of claim 5 wherein said integrated coplanar waveguide of said differentiation means has first and second ground planes and further comprises means for shorting said first and second ground planes together at a point such that said intermediate pulses have a round trip travel time from the point of coupling to said nonlinear transmission line to the point where said first and

second ground planes are shorted together and back again is substantially equal to said second rise time.

7. The apparatus of claim 6 wherein said RF waveguide means is an integrated coplanar waveguide having a center conductor and first and second ground plane conductors separated and electronically isolated from said center conductor, all formed on said surface.

8. The apparatus of claim 7 wherein said first and second ground planes of said differentiation means are the first and second ground planes of said RF waveguide means.

9. The apparatus of claim 8 wherein said first means further comprises a linear coplanar waveguide having a center conductor and first and second ground planes integrated on said surface and coupled to said nonlinear transmission so as to guide said intermediate pulses by coplanar waveguide propagation made to the point of coupling with said RF waveguide means, and further comprising coupling means for terminating said linear coplanar waveguide in its characteristic impedance and coupling said intermediate pulses to first and second ground planes only of said RF waveguide means to excite slot time mode propagation.

10. The apparatus of claim 9 wherein said coupling means comprises a 50 ohm resistor integrated in said substrate and coupling the center conductor of said linear coplanar waveguide of said first means to said first ground plane of said RF waveguide means and wherein said coupling means further comprises coincidence between said first and second ground planes of said linear coplanar waveguide of said first means and said second groundplane of said differentiation means.

11. The apparatus of claim 9 wherein said sampling means include first and second diodes integrated on said one surface, each said diode having an anode and a cathode, and further comprising first and second capacitors integrated on said one surface, said bottom plate of said first capacitor coupled to said first ground plane of said RF waveguide means and said top plate of said first capacitor coupled to said cathode of said first diode, and said anode of said first diode and said cathode of said second diode coupled to said center conductor of said RF waveguide means, and said anode of said second diode coupled to said top plate of said second capacitor, and said bottom plate of said second capacitor coupled to said second ground plane of said RF waveguide means, and further comprising a resistor having first and second terminals, said first terminal coupled to the cathode of said first diode and said second terminal coupled to the anode of said second diode and having a centertop terminal located so as to have

equal resistance between said centertop terminal to each of said first and second terminals, said centertop terminal serving as an output terminal at which an output signal occurs which has the same shape and voltage of said signal propagating on said RF waveguide means but at a substantially lower frequency.

12. An integrated sample head for generating an equivalent time low frequency reproduction of a high frequency periodic signal by sampling, comprising:

a substrate of semiconductor material having at least first and second sides;

sample pulse generation means integrated on said first side of said substrate as a coplanar waveguide for receiving sample pulses having a first rise time and for altering the shape of said sample pulses so as to have a rise which is shorter than said first rise time and for presenting said shape altered sample pulses at an output;

means integrated on said first side of said substrate and coupled to said output for differentiating said sample pulses appearing at said output;

an RF coplanar waveguide integrated on said first side of said substrate and having first and second ground plane conductors and a center conductor and an input;

a first diode/capacitor pair integrated on said first side of said substrate and coupled in series between said center conductor and said first ground plane conductor to form a first shunt path, said diode having an anode coupled to said center conductor and having a cathode coupled to said capacitor of said diode/capacitor pair;

a second diode/capacitor pair integrated on said first side of said substrate and coupled in series between said center conductor and said second ground plane conductor to form a second shunt path, said diode having a cathode coupled to said center conductor and having an anode coupled to said capacitor of said diode/capacitor pair;

a resistor integrated on said first side of said substrate having first and second end terminals coupled, respectively, to said cathode of said diode in said first diode/capacitor pair and said anode of said diode in said second diode/capacitor pair and having a centertap; and
an output terminal coupled to said centertap of said resistor.

13. An integrated sample head for generating an equivalent time low frequency reproduction of a high frequency periodic signal by sampling, comprising:

a substrate of semiconductor material having at least first and second sides;

a nonlinear coplanar sample pulse transmission line integrated on said first side of said substrate and having an input for receiving sample pulses having

a first rise time and having an output at which appears output sample pulses having a second, faster rise time than said first rise time;

a coplanar RF transmission line integrated on said first side of said substrate and having first and second ground plane conductors integrated on said first side of said substrate and separated by a semi-insulating region and having a center conductor integrated on said semi-insulating region of said substrate between said ground plane conductors and having an input for receiving said high frequency periodic signal to be sampled;

a coplanar sample pulse injection transmission line integrated on said first side of said substrate and having an input coupled to receive said output pulses from said sample pulse transmission line and having two ground plane conductors integrated on said first side of said substrate and separated by a semiinsulating region and having a center conductor integrated on said semiinsulating region of said substrate between said ground plane conductors;

means integrated on said first side of said substrate for terminating said coplanar sample pulse injection transmission line in its characteristic impedance and coupling signals propagating therein into said two ground plane conductors of said RF transmission line at a first location to excite the slot line mode thereof;

an air bridge conductor integrated on said first side of said substrate and shorting said first and second ground plane conductors of said RF transmission line at a second location removed from said first location by a distance which results in a round trip transit time of a pulse injected at said first location to said second location and back to said first location equal to the rise time of the output pulses from said sample pulse transmission line;

a first capacitor integrated on said first side of said substrate and having a top plate and a bottom plate coupled to said first ground plane conductor of said RF transmission line;

a second capacitor integrated on said first side of said substrate and having a top plate and a bottom plate coupled to said second ground plane conductor of said RF transmission line;

a first Schottky diode integrated on said first side of said substrate and having an anode coupled to the center conductor of said RF transmission line and having a cathode coupled to said top plate of said first capacitor;

a second Schottky diode integrated on said first side of said substrate and having an anode coupled to said top plate of said second capacitor and having a cathode coupled to said center conductor of said RF transmission line; and

a resistor integrated on said first side of said substrate having a first end terminal coupled to said

top plate of said first capacitor and having a second end terminal coupled to said top plate of said second capacitor.

5

10

15

20

25

30

35

40

45

50

55

MMIC Process August 5, 1988 RM

This process is for fabrication of the millimeter-wave transmission lines and schottky varactor diodes of a nonlinear transmission line pulse compressor; similar millimeter-wave circuits can be made with small process variations. Etch times and ion implant energies given are for the standard material for the nonlinear transmission line, ie a $0.6 \mu\text{m}$ N- layer (3×10^{16}) above a $0.8 \mu\text{m}$ N + layer (6×10^{18}) on a [100] semi-insulating GaAs substrate.

Process steps have subsequently been added to fabricate capacitors and air-bridges. These processes are still under development.

Fri, Sep 30, 1988

Page 1

APPENDIX A

Self-Aligned Ohmic Contacts

MASK LEVEL 1 DARK FIELD

In this step the N- layer is first etched to expose the N+ layer. Ohmic metal is then evaporated and lifted off using the same photoresist which served as an etch mask. The alignment marks are also on this mask layer.

Photoresist

Use AZ 5214 and follow standard photoresist procedure but postbake 120°C, 20 min, and USE HMDS

HMDS is not essential on GaAs but can be useful when adhesion is critical

After postbake, Alpha Step to find starting resist thickness

The resist thickness was found to be 1.55-1.65 microns

Verify resist thickness before etching!

Wet Etch

Use NH₄OH:H₂O₂:H₂O (14 : 2.4 : 200)

A 1:1 H₂O:H₂O₂ adjusted to PH 7.1 with NH₄OH has been shown to have less lateral etching.

Etch in H₂O bath for stable temperature.

Etch rate estimated at 0.44µm/min

Etch first piece for 1 min to establish etch rate

Stop etch with 2 min DI H₂O rinse, Nitrogen dry

Alpha Step to find the estimated etch depth

measure in two places

Don't forget to subtract the resist thickness

Perform additional wet etchs to get 0.75 µm etch depth

Estimate needed time conservatively to avoid overetching

Alpha Step after each etch to monitor progress

Evaporate Metal

Etch wafer for 60 seconds in 6:1 BOE immediately prior to evap.

Evaporate

108 Å Ge

102 Å Au

63 Å Ge

236 Å Au

100 Å Ni

6000 Å Au

Standard Liftoff

make sure periphery lifts off, otherwise it burn in the RTA

3-solvent clean, DI rinse...

Alloy metal at 450°C for 25 seconds in RTA
Measure Contact resistance

Fri, Sep 30, 1988

Page 3

Proton Implant

MASK LEVEL 2

DARKFIELD MASK CRITICAL ALIGNMENT

Proton implantation is used to electrically isolate N+ regions and to eliminate conductive layers under transmission lines. Protons are implanted into the wafer at high energies, generating ≈ 3 defect per proton & making the substrate semi-insulating. A thick Au layer defined by liftoff above a polyimide removal layer forms the implant mask.

Proton implant energies and doses depend on the particular layer structure and application.

Hot Solvent Clean**Apply Ciba-Geigy polyimide**

Spin adhesion promoter at 5000 rpm for 30 sec

Spin Probimide 286 at 5000 rpm for 30 sec

Bake polyimide

Bake at 100°C for 30 min

Ramp to 180°C, Hold for 15 min at 180 \pm 5°C

Ramp to 240°C, Hold for 15 min at 240 \pm 5°C

Let oven cool down to 150°C before removing wafers

Photoresist**Thick Metal liftoff with AZ 5214e**

Spin at 2500 rpm for 30 sec to achieve approx 1.95um

Increase exposure time by about 15%

This compensates for low reflectivity of the polyimide and the additional resist thickness. At 16.5mW/cm² with UV400 optics, the exposure time is 3.5 sec (58mJ/cm²).

Evaporate Metal

100A Ti

1.8um Au

Leave at least 1000A between the top of the Au and the top of the photoresist for safety.

Liftoff Metal

Soak in acetone for at least 30 min

One method that has worked is to give Lance or Tom (whoever is doing the deposition) a beaker and instruct him to put the wafer in a covered beaker of acetone when he is finished. You can then go in at your leisure, or even the next day to do the liftoff.

Swirl the acetone around to lift the metal.

If the metal refuses to lift, blast it with the acetone bottle.

Tom's spray gun can blast off unrelenting metal pieces

Since acetone attacks the seals of the spray gun, use water in the reservoir and periodically soak the wafer in acetone.

If absolutely necessary, Ultrasonic clean

Ultrasonic for as little time as possible

excess use can crack GaAs wafers and "unstick" deposited metals

Watch for liftoff of particular feature(s), then remove

Attenuate power by:

using large amounts of H₂O in Ultrasonic unit

using Teflon beaker to reduce chatter

dipping beaker only partially in the bath

Etch Polyimide

Etch in polyimide Etcher, QZ 3296, for 70 sec

Rinse in Etch Rinse, QZ 3297, for 30 sec

Rinse in DI H₂O for at least 30 sec

N₂ dry and inspect

Proton Implant

Send to IICO for Proton Implantation

IICO spectral services

3050 Oakmead Village drive

Santa Clara, CA 95051

408-727-2547

Small pieces to be implanted should be mounted on a 3" silicon wafer, using 3M brand Kapton tape

Implant Hydrogen

1e15 at 110keV and 2e15 at 190keV has been used for compensation of a 0.6um 3e16 N- layer on top of a 6e18 N+ layer.

Strip polyimide

Soak in hot (<=100C) polyimide thinner to remove gold

This takes at least 20min. One method that has worked is to soak 10min, ultrasonic 10 sec, soak 10 min, ultrasonic 10 sec, DI rinse immediately.

Ethylene diamine and ethanolamine are also available for use in stubborn cases. These are highly reactive solutions, and manufacturer's literature should be checked for instructions and safety precautions.

Use ultrasonic bath as necessary to aid in liftoff

see notes in "liftoff lithography" re use of ultrasonic
DI rinse, N2 dry

After removing wafer from the thinner, rinse immediately before the thinner has a chance to dry. This helps to prevent the lifted off gold from readhearing to the wafer.

Ash polyimide residue

Some edge residue may remain after mask removal

Ash at full power for 3 to 5 minutes to remove residue

Schottky and Interconnect Metal

MASK LEVEL 3 DARKFIELD MASK CRITICAL ALIGNMENT

This mask step replaces both the Schottky and interconnect metal steps. We put down thick (Ti/Pt/Au) metal on the transmission line pattern. Only where the substrate has been masked from proton isolation will a Schottky be formed- at all other points we get metal on insulating dielectric. Alignment is easier as we can misalign in the horizontal plane without making the metal miss the unimplanted regions, and a mask step is eliminated

Photoresist

Thick Metal Liftoff with AZ 5214 resist but:

...increase exposure $\approx 20\%$ to fully expose ohmic etch holes

... and develop in dark

Evaporate

Etch wafer in BOE for 60 secs prior to evaporation

Evaporate

1000 Å Ti

750 Å Pt

1.2 μ m Au

Liftoff

Silicon Nitride

Mask Level 4

DARKFIELD MASK

This dielectric layer serves two purposes. It is the capacitor dielectric, and it also protects the circuits from the atmosphere.

Surface Preparation

Solvent Clean (see above)

Trichlorethane

Acetone

Isopropyl

Rinse in cool DI water

Nitrogen blow dry

Dehydration bake 120 °C for 30 minutes

Let wafer cool 5-10 minutes

PECVD Si₃N₄

Typical capacitor dielectric thicknesses range from 0.10um to 0.25um. The very thin layers suffer yield problems on large area capacitors due to pin holes in the film. Thick layers tend to crack due to thermal expansion mismatch.

0.2um is probably a good place to start, but it would be nice to get down to 0.1um

Deposition temperature must be less than 290C. 250C is probably best.

Photoresist

Standard S1400-33 process

use adhesion promoter

hardbake 120C for 20 min

RIE

These instructions are for the Harris group machine.

The buttons on the machine have two states: in and out. The button should light when the button is depressed, unfortunately, most of the bulbs are burnt out, so you must look at the position of the switch to see if it is in or out.

PECVD/RIE switch

The same electronics are used to control both the PECVD and RIE machines, so be sure neither is in use before proceeding. If the PECVD/RIE key switch is on PECVD and no one is using it, turn the switch after disengaging the pump as described below.

Mains switch out

PECVD/RIE key switch to RIE

Mains switch in
Turn on gas bottles
Open valve on C2F6 bottle (normally open)
Pressure should be about 10psi
Put wafers in chamber
When not being used, the RIE chamber should be pumped down, therefore, it is necessary to purge and vent before hoisting the lid.
set purge timer to 1 min
purge 2 switch should be in
turn on both timers
vent switch in
after purge and vent, hoist up lid
Press both hoist up buttons simultaneously
vent switch out
arrange wafers
hoist lid down
Lower lid until it makes contact with the chamber all the way around.
If the lid is hoisted down to far, it will lift in the front. Once the lid is down, it may be necessary to align the lid with the chamber.
Switch to MPB pump for pump down
valve switch out
timers off
pump switch out
MPB switch in
pump switch in
valve switch in
wait for pressure to stop changing
Start gas flow
set pressure to zero with screwdriver
GAS2 switch in (C2F6)
Mode switch should be on open
flow on, adjust flow to 20
The flow is turned on with the toggle switch near the LED flow display for C2F6
The flow is adjusted with the 10 turn pot next to the toggle switch
log in to log book
The delay allows the gas to run at low pressure for a while to purge the chamber.

adjust pressure to 40mT

Pressure is adjusted with the 10 turn pot and multiplier switch near the LED pressure gauge.

mult switch set at 0.1

set mode to auto

The exit valve on the chamber will gradually close until the pressure is brought up to that specified.

slightly low reading on guage ok

ETCH

set process time

Etch rate is approx. 70A/min for sputtered nitride,
300A/min for PECVD nitride.

set purge time to 2.5 min

set RF power to 0W

RF power switch in

increase RF power to 200W in approx 2W out

The chamber can be matched either manually or automatically. Try auto mode first. Observe the reflected power as the input power is increased. If the reflected power is a significant fraction of the input power (>2%) the load needs to be matched. This is a two variable optimization process of 'tuning' and 'load'. If the load is set to auto, this should happen automatically, but rumor has it that the auto match doesn't always do the best job.

If there is extreme difficulty in matching the load (>30% reflected power), there is probably something wrong (like a conductive wafer bridging the anode to the cathode).

self bias should be 380V

When Process is Complete . . .

RF power shuts off automatically

Purge begins automatically

Set Mode switch to open

Turn off flow

Set RF power pot to 0

Wait for purge to finish

Vent switch in

When vent is completed the lid will raise slightly

Hoist lid, remove wafers

Vent switch out

Pump down

valve switch out

timers off

pump switch out

MPB

pump switch in

valve switch in

30 sec 6:1 BHF etch to clean up

Strip photoresist

Soak in acetone

Plasmod at full power for 5 min

RIE of Si₃N₄ tends to leave a thin polymer film that must be removed before subsequent processing steps. The plasmod will help ensure complete removal of this film.

Airbridge Posts

Mask Level 5 DARKFIELD MASK

There are two mask levels involved in making an airbridge. This mask level covers the area that is to be spanned by the bridge, but has holes where the bridge comes down to first level metal. Also, a hole is left where an MIM capacitor top-plate will be.

The airbridge process described here is adapted from a Texas Instruments process and a Hughes process. Chris Storment (723-1209 in AEL 132) gave me the information from Hughes, while John Owens of Santa Clara University explained the Texas Instruments process.

Photoresist

Use S1400-33 process for 3um thick film

AZ 5903 and AZ4330 are also being investigated

AZ5903 could provide taller bridges (up to 1.2mils!) and better aspect ratios (3:1), AZ4330 advertizes better aspect ratios (2:1) at similar thicknesses.

For best resolution use standard AZ5214 process
and hardbake 120C for 20min

Evaporate flash layer

This layer shorts all the airbridges together to provide a plating current path and also serves as a good surface on which to initiate plating. The layer must be thick enough to safely carry the plating current even over steps in the photoresist.

100A	Ti	sticking layer
2000A	Au	conductive layer
300A	Ti	sticking layer for subsequent photoresist.

The last layer also keeps the underlying gold surface clean until immediately prior to plating.

Procede to next level photoresist

Since it is impossible to do a solvent clean at this point, and any kind of an acid clean would be difficult (since the thin Ti layer etches in almost anything), it is advisable to put down the next layer of photoresist immediately after the wafer is removed from the vacuum chamber.

Airbridge Interconnects

Mask Level 6

DARKFIELD MASK

This is the second mask of the airbridge fabrication sequence. This mask defines the areas that will be up-plated with gold. Gold is plated to form airbridges and the top plates of MIM capacitors. This mask is a superset of the airbridge post mask. Anything feature defined by this mask but not on the previous mask will be suspended on top of the previous layer of photoresist.

Photoresist

Adhesion is critical in this step so be sure to use adhesion promoter

Be certain that there is no scum left. Scum can devastate this whole process.

Use AZ4330 process except . . .

softbake for 60min at 75C

expose for 16 sec at 16.5mW/cm² (265mJ/cm²)

develop in 1:1 H₂O:AZ concentrate. watch!

DUV expose?

It would be desirable at this point to do a 2min DUV expose instead of a hardbake which makes the lower layer more difficult to remove. Unfortunately, we do not currently have this capability.

Open areas for electrical contact to flash layer

Apply one drop of acetone to the lower left and upper right corners of the wafer. Let each drop stand until it has dissolved some photoresist then DI rinse and N₂ dry. Repeat until there is a nice clean clear area.

This is really not a good way to accomplish electrical contact. Putting these areas on the airbridge crossover mask would make more sense.

post-bake 30 min at 90C

AZ5903 and S1400-33 are also being investigated

Etch 300A Ti layer

Use 20:1 H₂O:HF solution

Etch until 10sec after wafer turns gold (approx 1min)

DI rinse N₂dry

Inspect under optical microscope.

The Au will not plate significantly on Ti and not at all on dirty Ti. Be sure Ti is completely cleared in regions to be plated.

Plate 1.8um Au or as much as you dare.

Due to the two layer photoresist structure it is difficult to resolve narrow spaces (think of the aspect ratio of the complete 2 layer feature). So beware. Currently, plating for 8min at 50mA is working well and yields about 1.8um in the finished structure.

2.3 um has been done with this process but 2.5um spaces are marginal.

Rinse off top layer of photoresist with acetone spray

Spraying instead of soaking prevents attacking the lower level resist. If things start lifting off now, it could get messy.

Rinse with isopropal and DI spray

Etch 2000A Au layer

Use KI₂:I₂:H₂O gold etch in lab diluted in 10 parts H₂O

RIE or Ion Milling would be superior ways to go if and when available.

Etch until 10 sec after Au clears.

This is very difficult to tell in this murky brown solution so check every 15 seconds by DI rinsing. It should take approximately 30 seconds.

DI rinse, N₂ dry.

Etch 100A Ti layer

This is certainly not necessary, however, it makes removal of the lower level photoresist easier.

Use 20:1 H₂O:HF solution

Etch approx 30 seconds

DI rinse N₂ dry

Strip lower level resist

This is difficult using acetone alone. The warm stripper hasn't been tried but should work better.

Soak in acetone

Soak in warm photoresist stripper

Do not ultrasonic

APPENDIX SECTIONS

Fri, Sep 30, 1988

Page 15

Wafer Cleaning

Be careful about boiling solvents. TCA and acetone both tend to boil in an unstable fashion, occasionally superheating and then expelling solvent all over the place at once. Use some source of nucleation for bubbles, like tweezers, stirring rod, etc.

In transferring the wafer between solvents, make sure that the surface remains wet at all times. In the final step, DI water rinse & nitrogen dry, the water should be blown off as a sheet, leaving no drops to dry, leaving a residue.

2 minutes in boiling TCA

2 minutes in Acetone at room temperature, or slightly warmed

Acetone is suspected to be weakly carcinogenic, so DON'T boil the stuff. If you do boil it, keep it under the hood.

2 minutes in boiling Isopropyl

DI water rinse

N2 dry

dehydration bake if photoresist or polyimide follows
120°C for 30min.

Mask Cleaning

...is essential for high-resolution, high-yield lithography if you plan to use your mask more than once

Soak in Shipley photoresist remover

very gentle wet scrubbing with Q-tip

DI rinse

Nitrogen dry

use air knife and be very careful not to drop the mask

Store waste in gallon jug for later disposal

Remover 150 is an organic acid and needs to be stored for proper disposal.

Remover 1165 is a mixture of solvents that can be disposed of down the solvent drain.

Standard AZ5214e Photoresist (etch masks, etc.)**Surface Preparation**

This section assumes that nothing has been done previously to the wafer. If processing has already occurred then it may be necessary to skip some cleaning steps so that the wafer is not damaged

Solvent Clean (see above)

Dehydration bake 120 °C 30 minutes

Let wafer cool 5-10 minutes

Photoresist application

Spin on adhesion promoter 40 sec 3000 rpm

adhesion promoter should be filtered

approx .75 cc per 2" wafer

Spin AZ 5214e for 40 seconds at 3000 rpm

approx 1.5 cc per 2" wafer

Soft Bake

Think about thermal inertia ! If you bake pieces in a closed petri dish, or in an open dish with large thermal mass, then bake times will have to be increased. Best to use open vessels.

Times given are for baking small pieces on an open petri dish on the top shelf of a Blue-M oven.

Bake in convection oven for 25 minutes at 90°C

Turn on Aligner so source can warm up

Let wafers cool (approx. 5 minutes)

Exposure

Log into logbook and follow directions for aligner

Expose 50 mJ with uv400 optics (3 sec at 16.5mW/cm²)

or expose 192 mJ with uv300 optics

Most properties of AZ5214e are better with uv400 optics. The one advantage of 300nm optics is the possibility of submicron resolution.

Development

Develop 90 seconds in 1:1 solution AZ developer:H₂O (watch)

use 2-beaker development with last 15 seconds in "clean" developer

Rinse in DI for 2 minutes

Nitrogen dry

Pour developer down the drain

Postbake

30min at 140C is necessary for the harshest applications

20min at 120C is recommended for most applications
20min at 90C is adequate if edge rounding is unacceptable
Gentle Plasma Descum, if necessary
Inspect wafers under optical microscope

S1400-33

This resist spins on in the neighborhood of 2.8um. Aspect ratios are no better than 1:1. Stability in PH 9.5 is reasonable with only a 30min 90C bake.

Surface Preparation

This section assumes that nothing has been done previously to the wafer. If processing has already occurred then it may be necessary to skip some cleaning steps so that the wafer is not damaged

Solvent Clean (see above)

Dehydration bake 120 °C 30 minutes

Let wafer cool 5-10 minutes

Photoresist application

Spin on adhesion promoter 40 sec 3000 rpm

adhesion promoter should be filtered

approx .75 cc per 2" wafer

Spin S1400-33 for 40 seconds at 3000 rpm

approx 1.5 cc per 2" wafer

Soft Bake

If you bake pieces in a closed petri dish, or in an open dish with large thermal mass, then bake times will have to be increased. Best to use open vessels.

Times given are for baking small pieces on an open petri dish on the top shelf of a Blue-M oven.

Bake in convection oven for 25 minutes at 90°C

Turn on Aligner so source can warm up

Let wafers cool (approx. 5 minutes)

Exposure

Log into logbook and follow directions for aligner

Expose 230 mJ with uv400 optics (14 sec at 16.5mW/cm²)

Development

Develop 50 seconds in 1:1 solution AZ developer:H₂O (watch)

use 2-beaker development with last 15 seconds in "clean" developer

Rinse in DI for 2 minutes

Nitrogen dry

Pour developer down the drain

Postbake

30min at 140C is necessary for the harshest applications

20min at 120C is recommended for most applications

20min at 90C is adequate if edge rounding is unacceptable

Gentle Plasma Descum, if necessary
2 min or less on full power in O₂ plasma using the plasmod
Inspect wafers under optical microscope

AZ4330

AZ4330 is a highly transparent photoresist with advertised aspect ratios of better than 2:1. It spins on in the neighborhood of 3.8um. This resist is one used by Hughes in their airbridge process. It is advertised to be stable in alkaline plating baths.

Surface Preparation

This section assumes that nothing has been done previously to the wafer. If processing has already occurred then it may be necessary to skip some cleaning steps so that the wafer is not damaged

Solvent Clean (see above)

Dehydration bake 120 °C 30 minutes

Let wafer cool 5-10 minutes

Photoresist application

Spin on adhesion promoter 40 sec 3000 rpm

adhesion promoter should be filtered
approx 0.75 cc per 2" wafer

Spin AZ4330 for 40 seconds at 3000 rpm

approx 1.5 cc per 2" wafer

Soft Bake

If you bake pieces in a closed petri dish, or in an open dish with large thermal mass, then bake times will have to be increased. Best to use open vessels.

Times given are for baking small pieces on an open petri dish on the top shelf of a Blue-M oven.

Bake in convection oven for 60 minutes at 90°C

There is a trade off here between soft bake time and contrast. The 60 min bake is supposed to give the best contrast. A shorter bake time would be acceptable but would reduce contrast.

Turn on Aligner so source can warm up

Let wafers cool (approx. 5 minutes)

Exposure

Log into logbook and follow directions for aligner

Expose 260 mJ/cm² with uv400 optics (16 sec at 16.5mW/cm²)

Development

Develop 130 seconds in 1:1 solution AZ developer:H₂O (watch)

develop time not yet established

use 2-beaker development with last 15 seconds in "clean" developer

Rinse in DI for 2 minutes

Nitrogen dry

Pour developer down the drain

Postbake

30min at 140C is necessary for the harshest applications

20min at 120C is recommended for most applications

20min at 90C is adequate if edge rounding is unacceptable

Gentle Plasma Descum, if necessary

2 min or less on full power in O2 plasma using the plasmod

Inspect wafers under optical microscope

AZ5903 (Under Development)**Surface Preparation**

This section assumes that nothing has been done previously to the wafer. If processing has already occurred then it may be necessary to skip some cleaning steps so that the wafer is not damaged

Solvent Clean (see above)

Dehydration bake 120 °C 30 minutes

Let wafer cool 5-10 minutes

Photoresist application

Spin on adhesion promoter 40 sec 3000 rpm

adhesion promoter should be filtered

approx .75 cc per 2" wafer

Apply and Spread AZ5903 for 20 seconds at 100 rpm

This resist is too thick to use the usual in line filter.

approx 4cc per 2" wafer

Spin at 6000 rpm for 100 sec for 8um thickness

Edge bead removal?

Soft Bake

If you bake pieces in a closed petri dish, or in an open dish with large thermal mass, then bake times will have to be increased. Best to use open vessels.

Times given are for baking small pieces on an open petri dish on the top shelf of a Blue-M oven.

Thick resists will crack during exposure if not well baked

Bake in convection oven for 40 minutes at 90°C

Turn on Aligner so source can warm up

Let wafers cool (approx. 5 minutes)

Hold for >10 min but < 2hrs

Exposure

Log into logbook and follow directions for aligner

Expose 660 mJ with uv400 optics (40 sec at 16.5mW/cm²)

Development

Develop 120 seconds in 1:1 solution AZ developer:H₂O (watch)

use 2-beaker development with last 15 seconds in "clean"

developer

Rinse in DI for 2 minutes

Nitrogen dry

Pour developer down the drain

Postbake

Postbake should be within 5 to 10C of the softbake temp or the resist will flow significantly (at higher temperatures).

40min at 90C

Gentle Plasma Descum, if necessary

2 min or less on full power in O2 plasma using the plasmod

Inspect wafers under optical microscope

Liftoff Photoresist (Metallization)

Let's talk a little about liftoff lithography and lithography in general. A number of difficulties arose in making a Chlorobenzene liftoff process for the Suss aligner, and we learned a number of things in the process.

The idea in liftoff lithography is to generate resist with overhanging edges. Metal deposition from some point source (e.g. an electron-beam evaporator) will then result in a film which is discontinuous over resist edges. Dissolution of the resist in Acetone or resist thinner will then remove all metal over the resist, leaving only metal that was deposited on the semiconductor substrate. Overhanging edges are critical!!!

To attain such edges we do two things: we harden the surface of the resist with Chlorobenzene and we SOFTEN the underlying resist by incomplete softbaking. Ideally, resist will not develop in areas where it has not been exposed; all practical resists have some small development rate even if unexposed. By under-baking the resist during softbake, significant dissolved solvents and water will remain in the resist, increasing the unexposed development rate. Underbaking introduces problems, as development times are reduced and become sensitive to the exact bake conditions. In combination with a resist surface which has been in some way hardened, development will occur more rapidly in the depth of the resist than on the surface, generating an undercut edge profile. The edges of the resist then will have an overhanging lip, plus some recessed sidewall, whose slope may be vertical or either inward or outward.

The lip is generated by surface hardening with a Chlorobenzene soak. This process is neither high-resolution nor terribly reproducible; we simply are using it until a more sophisticated 2-resist process is developed. Chlorobenzene selectively removes lighter (low molecular weight) polymers from the resist, leaving a resist surface which then dissolves more slowly in developer. As longer soaks permit progressively deeper penetration of the Chlorobenzene solvent, the vertical thickness of the resist is a function of the soak time. Fifteen minutes gives a good thick lip ($\approx 0.2 \mu\text{m}$) which doesn't seem to wilt under exposure to high temperatures during metal evaporation. Process reproducibility is also most likely improved with longer chlorobenzene soak times.

The slope of the recessed sidewall can be important. The ideal profile is a slight outward slope, so that the overhanging lip of the resist is directly above the bottom edge of the resist where it meets the substrate. This permits most accurate dimensional control and allows for accurate registration of recess etch and deposited metal in self-aligned gate processes. If the edge slope is severe, so that the bottom edge of the resist projects beyond the lip, then control of metallization feature size is lost. In severe cases, the slope can be so poor that a continuous metal film is deposited during evaporation, preventing liftoff.

Edge slope is well correlated to resist actinic absorbance and to exposure time. To understand this better, we really need to look at the contrast curves of the resist; these are much like the contrast curves of photographic film. Ideal photoresist would dissolve away (develop) at zero rate at all exposure energies below some threshold energy E_{th} , and etch away at a high rate for exposures above E_{th} . Practical resist shows fast development at exposures above E_{th} , but the exposure rate then decreases at some finite rate for exposures below this- the faster the decrease in exposure rate the higher the resist's CONTRAST (gamma). Now, photoresist is not perfectly transparent. The transparency increases as the resist is exposed, and the difference between the unexposed and exposed absorption coefficients is called the actinic absorbance. If the attenuation is significant, the exposure at the bottom of the photoresist will be lower than at the top. If the exposure at the top of the resist is near E_{th} , then the exposure at the bottom of the resist will be below E_{th} , decreasing the development rate at the bottom and thus generating sloping edges. The solution is then to increase the exposure slightly. Clearly, resists with lower attenuation show less of an edgwall slope problem.

For this reason, lithography with 1400 or 1300 series resists (Shipley or Hoescht) is not advisable on the Karl Suss aligner operating at 300 nm. The attenuation coefficient of these resists at 300 nm is about 1.5 nepers/micron, and the resulting sidewalls are sloped at about 45 degrees! Hoescht resist AZ 5200-series has much better transparency at 300 nm, and permits near-vertical sidewalls at 300 nm exposure. Sidewall slope is adjusted by varying the exposure time. AZ-5200 resists are generally just more modern than the 1400 and 1300 series, and have a number of other improved properties, including improved dimensional control during hardbake.

Surface Preparation

Solvent Clean (see above)

Trichlorethane

Acetone

Isopropyl

Rinse in cool DI water

Nitrogen blow dry

Dehydration bake 120 °C for 30 minutes

Let wafer cool 5-10 minutes

Photoresist application

Spin adhesion promoter for 40 seconds at 3000 rpm

Spin AZ 5214e photoresist for 40 seconds at 3000 rpm

spin at less than 3000 rpm for thickest metals

Clean and turn off Spinner

Soft Bake

Think about thermal inertia ! If you bake pieces in a closed petri dish, or in an open dish with large thermal mass, then bake times will have to be increased. Best to use open vessels.

Times given are for baking small pieces on an open petri dish on the top shelf of a Blue-M oven.

Bake in convection oven for 25 minutes at 75 °C

Turn on Aligner so source can warm up

Let wafers cool (approx. 10 minutes)

Exposure

Log into and follow direction on the aligner
align if necessary (possible?)

Expose for 50 mJ (3 sec at 16.5mW/cm²)

Chlorobenzene

Soak the wafer for 15 minutes in undiluted chlorobenzene

Chlorobenzene should be used in a covered beaker at the rear of the laminar flow hood to prevent fumes from entering the room.

Nitrogen dry the wafers

Pour chlorobenzene in special container

When full, the waste chlorobenzene can be disposed of in the solvent disposal drum in the Ginzton Lab north courtyard.

Development

Develop 1.5 to 1.75 minutes in 1:1 AZ solution developer:H₂O
(watch)

We (MR & CM) have decided that the best method here is to watch the development. When large (visible) areas on the wafer have cleared, transfer to the "clean" beaker for the final 15 seconds.

two-beaker method: last 15-30 seconds in "clean" beaker of developer

Rinse in DI water for 2 minutes

Nitrogen dry

Pour developer down the drain

Pre-evaporation clean

Just before placing wafers in evaporator do a 60 second buffered oxide etch in a teflon beaker. BOE contains HF, so be sure to dispose of it in the waste HF mixtures container.

Evaporate desired metal(s)

Liftoff Metal

Resist temptation to attack the metal. The best lift off tool is time and patience. Let the wafer sit at the bottom of the beaker for an hour or so.

Soak in acetone for at least 60 min

One method that has worked is to give Lance or Tom (whoever is doing the deposition) a beaker and instruct him to put the wafer in a covered beaker of acetone when he is finished. You can then go in at your leisure, or even the next day to do the liftoff.

Swirl the acetone around to lift the metal.

If the metal refuses to lift, blast it with the acetone bottle.

Tom's spray gun can blast off unrelenting metal pieces

Since acetone attacks the seals of the spray gun, use water in the reservoir and periodically soak the wafer in acetone.

If absolutely necessary, Ultrasonic clean

Ultrasonic for as little time as possible

excess use can crack GaAs wafers and "unstick" deposited metals

Watch for liftoff of particular feature(s), then remove

Attenuate power by:

using large amounts of H₂O in Ultrasonic unit

using Teflon beaker to reduce chatter

dipping beaker only partially in the bath

Acetone, isopropyl, and DI water rinse

N₂ dry wafers

Inspect in optical microscope

Gold Plating

Since plating is a selective, additive procedure, it is potentially much more economical than subtractive methods such as sputtering and evaporation which coat the entire inside of the vacuum chamber.

However, plating tends to be a lower resolution process than other methods because it follows the contours of the resist which is defining the region to be plated. This means the line width is determined not by the width of the resist space at the bottom near the substrate, but by the width of the space at whatever level the gold is plated.

Put teflon base in the 3 liter beaker.

Use 1/2 gallon of Sel-Rex Neutronix 309 gold plating solution.

The solution can be reused until the gold is depleted unless it is contaminated.

Unused solution is clear.

Insert anode into base.

Heat solution to 50C

Use Lance's hot plate with the stir-bar motor. Put heat on 7 until the solution reaches 40C then reduce to 3.5 to maintain temperature at 50C. Watch to make sure the solution does not boil. It may be necessary to back off on the heat a little during the initial warm-up.

Plating at an improper temperature can result in gold being REMOVED from the wafer.

Put wafer on holder and insert into base.

The two gold spring clips should make good electrical contact to the cleared gold areas on the wafer. The wafer should be flat in the 5mil recess in the holder.

Hook ground to wafer contact wire, plus to anode wire.

Plate, agitating vigorously

The specified current density is 4 amps per square foot. (4.3 mA/cm²). However, you must account for the fact that you are plating a good deal of wire also. The current will most likely be experimentally determined. 50mA for a 2" wafer is a good place to start.

Plating too fast will result in dark, ugly deposits.

Turn stir bar speed up until just before a vortex is formed (about 7 on Lances hot plate).

Remove wafer holder. DI rinse, N2 dry wafer.

Filter plating solution as it is poured back into container.

Rinse the plating apparatus

Appendix A B

$$[1] \quad Z_0(V) = \sqrt{L/C_T(V)}$$

Various parameters of interest:

$Z_0(V)$ = the small-signal characteristic impedance of the transmission line as a function of voltage, V ,

$L = Z_1 \tau$ = inductance of the interconnecting transmission lines, per section,

$C_T(V)$ = the total capacitance per section as a function of voltage,

V = the instantaneous voltage at any particular point on the line,

$\tau = (P/c_0)\sqrt{(1 + \epsilon_r)/2}$ = the electrical spacing of the Schottky varactor diodes in time units,

P = the electrical spacing of the Schottky varactor diodes in distance units,

ϵ_r = dielectric constant of gallium arsenide ≈ 12.5 ,

c_0 = speed of light in vacuum,

Z_1 = characteristic impedance of the interconnecting transmission line.

$$[2] \quad C_T(V) = [C_j(V) + C_L] = \text{total capacitance per section,}$$

where,

$$[3] \quad C_L = \tau/Z_1 = \text{the capacitance of the interconnecting transmission lines, per section,}$$

and,

$$[4] \quad C_j(V) = C_{j0}/\sqrt{1 - V/\phi} = \text{the transition capacitance of a step junction diode with a junction potential } \phi, \text{ where in the preferred embodiment, } C_{j0} = 50\text{fF at } 160\mu\text{m spacings along a } 90\Omega \text{ coplanar waveguide transmission line, and } \phi \simeq 0.8 \text{ volts.}$$

$$[5] \quad T(V) = \sqrt{LC_T(V)}$$

where,

$T(V)$ = the group delay of the transmission line.

$$[6] \quad \omega_{per} \simeq 2/\sqrt{L(C_{ls} + C_L)} = 2/[Z_{ls}(C_{ls} + C_L)],$$

where C_{ls} is defined by equation (10) and Z_{ls} is defined by equation (12).

$$[7] \quad \omega_{rc} = 1/r_s C_j(V) \approx 1/r_s C_{ls},$$

where,

r_s = the varactor series resistance $\approx 10\Omega$.

$$[8] \quad T_{f,out} \simeq \max \left\{ \begin{array}{l} T_{f,min}, \\ T_{f,in} - n[T(V_h) - T(V_l)] \end{array} \right\}.$$

where,

n = the number of sections in the transmission line, and V_h and V_l are the high-level voltage and low-level voltage of the input signal.

$$[9] \quad Z_1 C_{ls} \omega_{per} \sin(\omega_{per} \tau) / 2 = \cos(\omega_{per} \tau) + 1,$$

where,

$$[10] \quad C_{ls} = \frac{[Q(V_h) - Q(V_l)]}{(V_h - V_l)},$$

where in the preferred embodiment, $C_{ls} \gg C_l$.

$$[11] \quad V_{out}(t) = V_{in}[t - nT(V)],$$

where $T(V)$ is given by equation (5) above.

$$[12] \quad Z_{ls} = \sqrt{\frac{L}{C_{ls} + C_l}}$$

$Z_{ls} \simeq 50\Omega$ for a 0 to -2 volt step-function input with the structure of Figures 2 and 4 on a 90Ω coplanar waveguide loaded by 45 diodes with $10\mu\text{m} \times 10\mu\text{m}$ junction area on an N-layer doped to $3 \times 10^{16}/\text{cm}^3$ at $160\mu\text{m}$ spacings.

Process for Fabrication of Nonlinear Transmission Lines

This process is for fabrication a nonlinear transmission line pulse compressor; starting material for the nonlinear transmission line is a $.6 \mu\text{m}$ N- layer (3×10^{16}) above a $.8 \mu\text{m}$ N + layer (3×10^{18}) on a [100] semi-insulating GaAs substrate.

Self-Aligned Ohmic Contacts

In this step the N- layer is first etched to expose the N+ layer. Ohmic metal is then evaporated and lifted off using the same photoresist which served as an etch mask. The alignment marks are also on this mask layer.

Photoresist

Use AZ 5214 and follow standard photoresist procedure (attached)

resist thickness: $1.55\text{--}1.65 \mu\text{m}$

Wet Etch

Use $\text{NH}_4\text{OH}:\text{H}_2\text{O}_2:\text{H}_2\text{O}$ (14 : 2.4 : 200) in room-temperature H_2O bath

Etch to $0.75 \mu\text{m}$ depth

Evaporate Metal

Etch wafer for 60 seconds in 6:1 BOE immediately prior to evap.

Evaporate

500 Angstroms Eutectic (88%-12%)Au-Ge

100 Angstroms Ni

2000 Angstroms Au

Lift Off

Soak wafers 30 min in cool acetone

spray with acetone to remove metal

If necessary, Ultrasonic clean to remove metal residue

Acetone, isopropyl, and DI water rinse

N_2 dry wafers

Alloy metal at 450°C for 12 seconds in Rapid Thermal Annealer

Proton Implant

Proton implantation is used to electrically isolate N+ regions and to eliminate conductive layers under transmission lines. Protons are implanted into the wafer at high energies, generating ≈ 3 defect per proton & making the substrate semi-insulating. A thick Au layer defined by liftoff above a polyimide removal layer forms the implant mask.

Wafer clean as per below

Apply Ciba-Geigy polyimide

Spin polyimide adhesion promoter at 5000 rpm for 30 sec

Spin Probimide® 286 at 5000 rpm for 30 sec

Bake polyimide

Bake at 100°C for 30 min

Ramp to 180°C, Hold for 15 min at 180 +/- 5°C

Ramp to 240°C, Hold for 15 min at 240 +/- 5°C

Let oven cool down to 150°C before removing wafers

Photoresist

Follow the "Liftoff photoresist" procedures

Increase exposure time by about 10% to compensate for the low reflectivity of polyimide.

Evaporate Metal

100Å Ti

1.6µm Au

Lift Off Metal

Soak wafers 30 min in cool acetone

spray with acetone to remove metal

If necessary, ultrasonic clean to remove metal residue

Acetone, isopropyl, and DI water rinse

N2 dry wafers

Etch Polyimide

Etch in polyimide Etcher, Ciba-Geigy QZ 3296, for 150 sec

Rinse in Etch Rinse, Ciba-Geigy QZ 3297, for 30 sec

Rinse in DI H2O for at least 30 sec

N2 dry

Implant Hydrogen, 7E14/cm² at both 110 and 160 keV

Strip polyimide and gold

Soak in hot polyimide thinner (Ciba-Geigy) to remove gold and polyimide

Use ultrasonic bath as necessary to aid in removal

Ash polyimide residue in oxygen plasma asher

Ash at low - medium power

Schottky and Interconnect Metal

This mask step replaces both the Schottky and interconnect metal steps. We put down thick (Ti/Pt/Au) metal on the transmission line pattern. Only where the substrate has been masked from proton isolation will a Schottky be formed- at all other points

we get metal on insulating dielectric.

Photoresist

Follow "Liftoff Photolithography directions but:

...increase exposure $\approx 20\%$ to fully expose ohmic etch holes

... and develop in dark

Evaporate

Etch wafer in BOE for 60 secs immediately prior to evaporation

Evaporate

1000 Å Ti

750 Å Pt

1.4 μm Au

Lift Off

Soak wafers 30 min in cool acetone

spray with acetone to remove metal

If necessary, ultrasonic clean to remove metal residue

Acetone, isopropyl, and DI water rinse

N₂ dry wafers

Processing: Appendix Sections

Wafer Cleaning

2 minutes in boiling Trichloroethane

2 minutes in hot Acetone

2 minutes in boiling Isopropyl

DI water rinse

Nitrogen dry

dehydration bake 120°C 30 minutes

Standard Photoresist

Surface Preparation

Solvent Clean (see above)

Dehydration bake 120 °C 30 minutes

Let wafer cool 5-10 minutes

Photoresist application

Spin AZ 5214e for 40 seconds at 3000 rpm

Soft bake in convection oven for 25 minutes at 90°C

Times given are for baking small pieces on an open petri dish on the top shelf of a Blue-M oven.

Expose 13 sec @14.8 mW/cm² on the Suss aligner for AZ 5214e

This formulation is for 300 nm exposure on the Suss through a BOROSILICATE mask.

Development

Develop 50 seconds in 1:1 solution AZ developer: H₂O

Development may have to be done in the dark if two distinct metallizations are on the substrate (battery effect).

use 2-beaker development with last 15 seconds in "clean" developer

Rinse in DI for 2 minutes

Nitrogen dry

Postbake 90°C, 30 minutes

Liftoff Photoresist (Metallization)

Clean Wafer (see above)

Spin AZ 5214e photoresist for 40 seconds at 3000 rpm

Soft bake in convection oven for 25 minutes at 75 °C

Time given is for baking small pieces on an open petri dish on the top shelf of a Blue-M oven.

Align and expose

For Suss at 310 nm exposure: 13 Seconds @ 14.8 mW/cm² through borosilicate mask.

Chlorobenzene

Soak for 15 minutes in undiluted chlorobenzene

Nitrogen dry

Development

Develop 1.5 to 1.75 minutes in 1:1 AZ solution developer: H₂O (watch)

We (MR & CM) have decided that the best method here is to watch the development. When large (visible) areas on the wafer have cleared, transfer to the "clean" beaker for the final 15 seconds.

two-beaker method: last 15-30 seconds in "clean" beaker of developer

Rinse in DI water for 2 minutes

Nitrogen dry

Pre-evaporation clean

Just before placing wafers in evaporator, do a 60 second buffered oxide etch in a teflon beaker.

Evaporate desired metal(s)

Lift Off

Soak wafers 30 min in cool acetone
spray with acetone to remove metal
If necessary, ultrasonic clean to remove metal residue
Acetone, isopropyl, and DI water rinse
N2 dry wafers

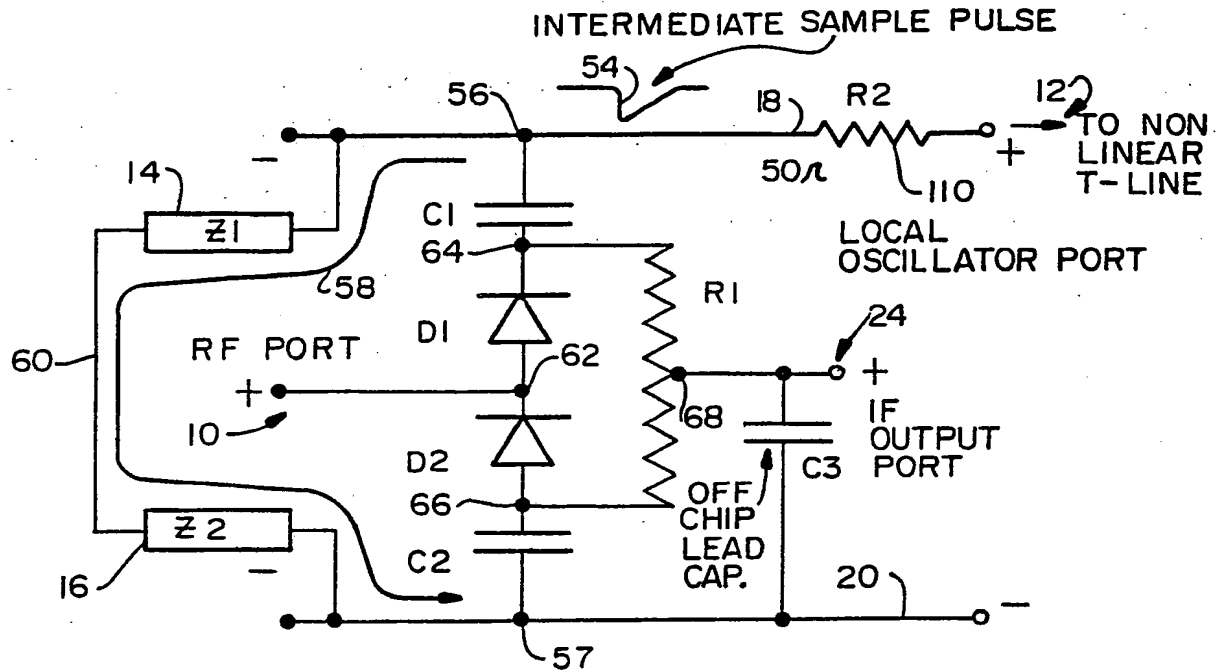


FIG. 1

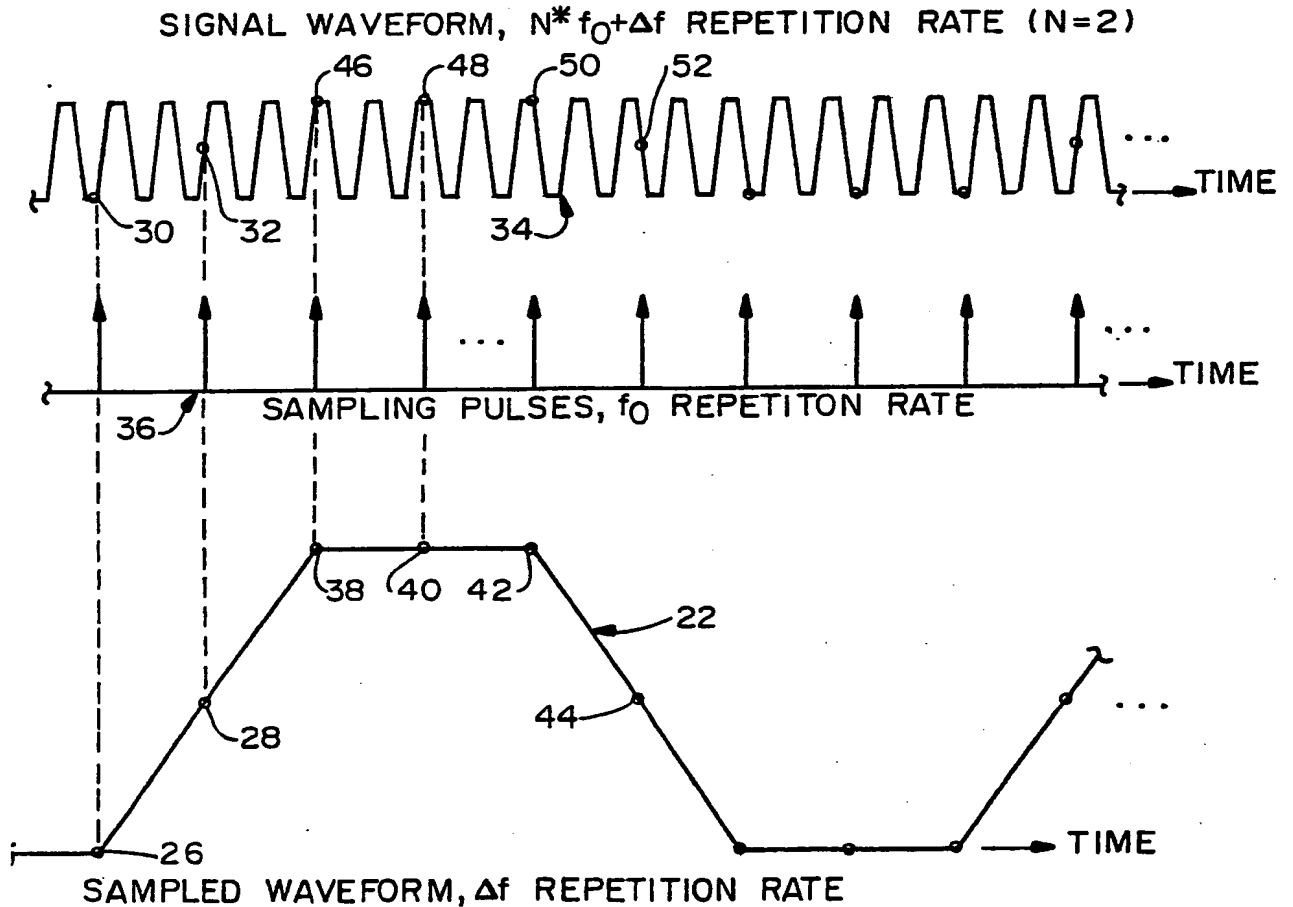


FIG. 2

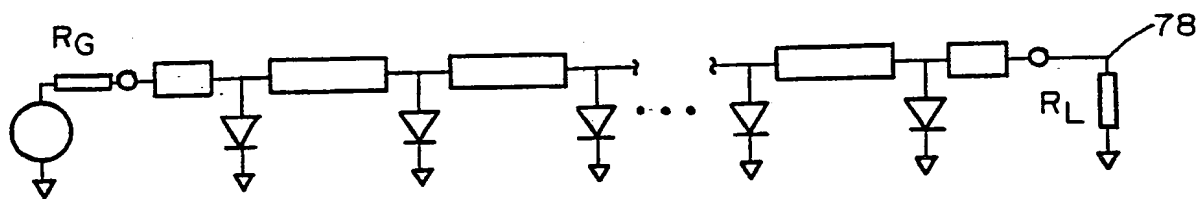


FIG. 3

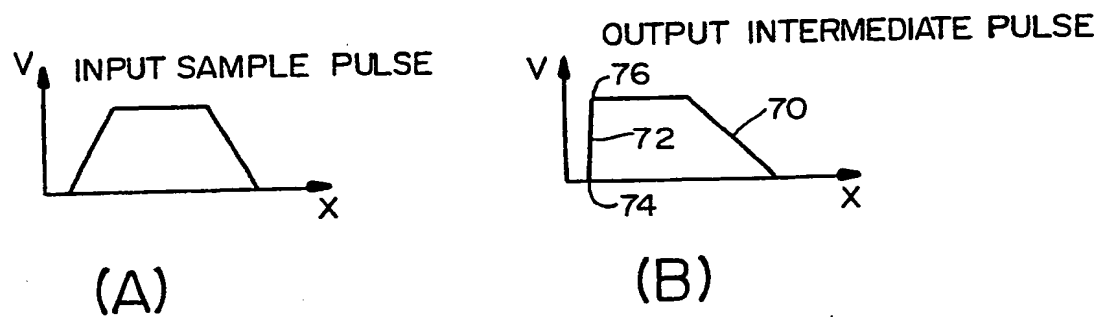


FIG. 4

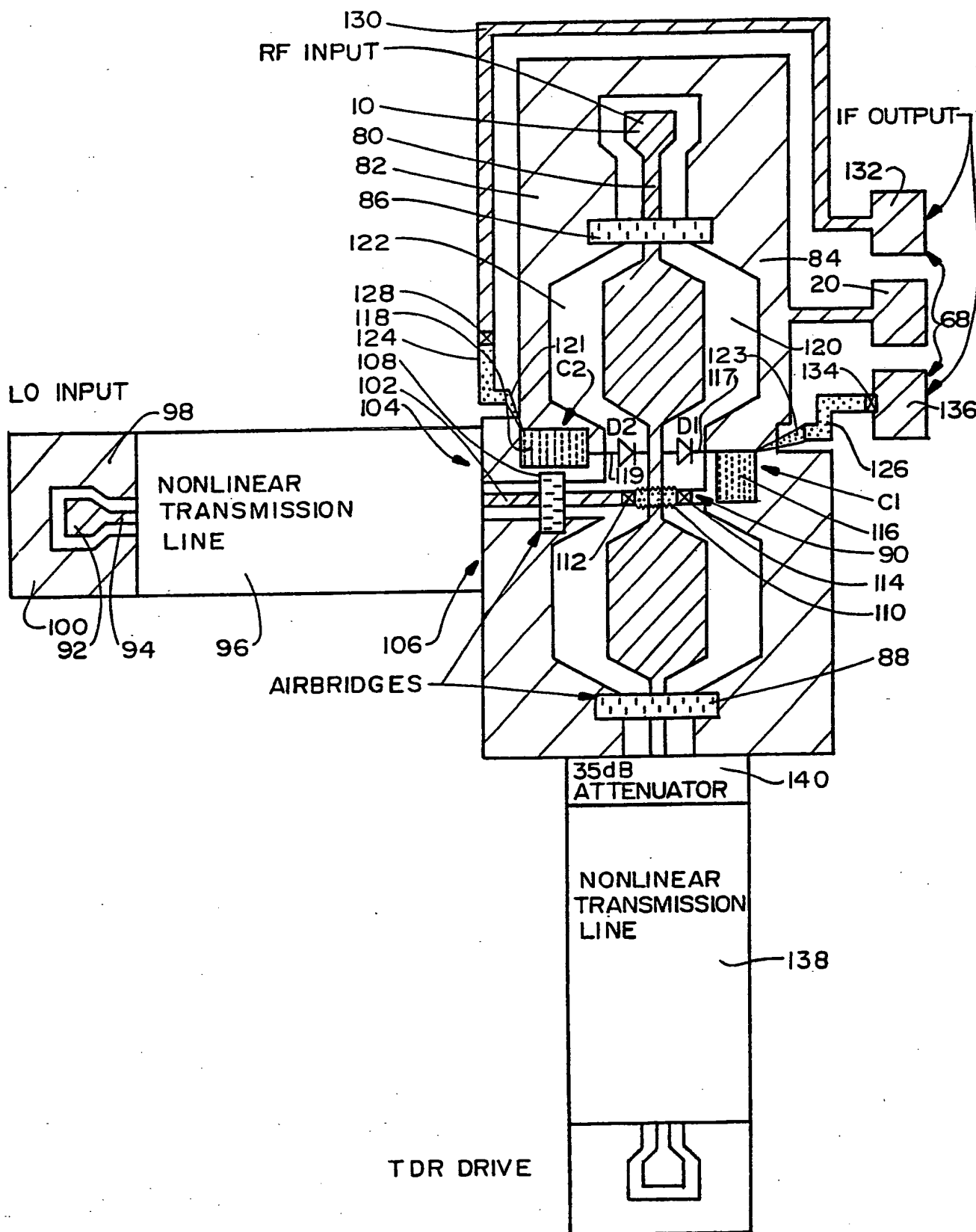
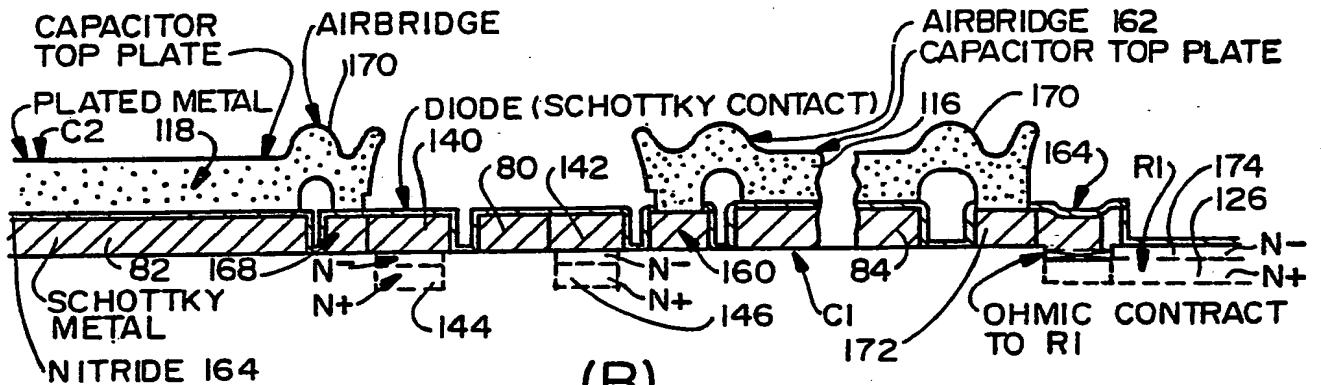


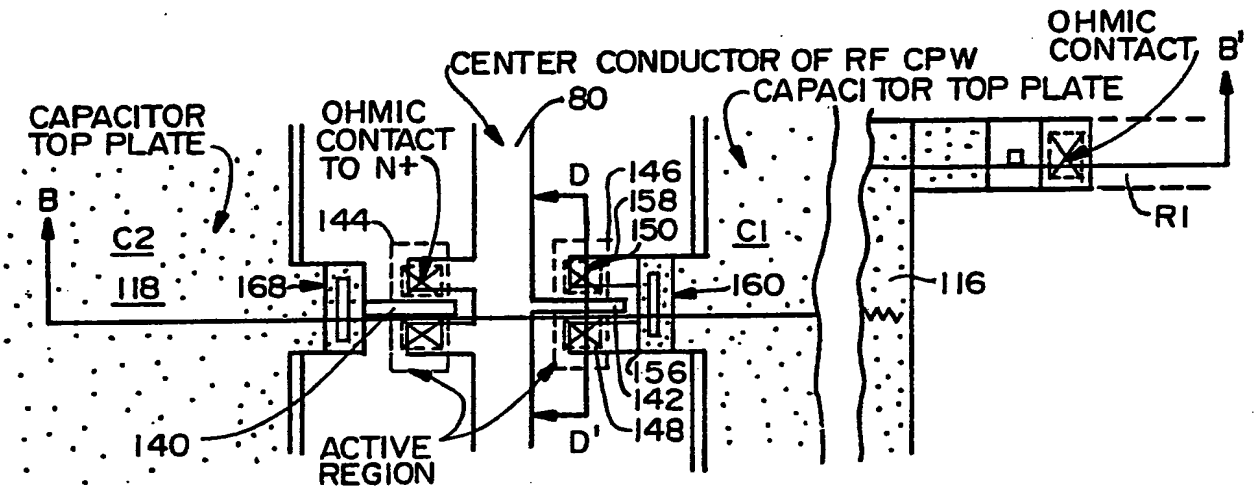
FIG. 5



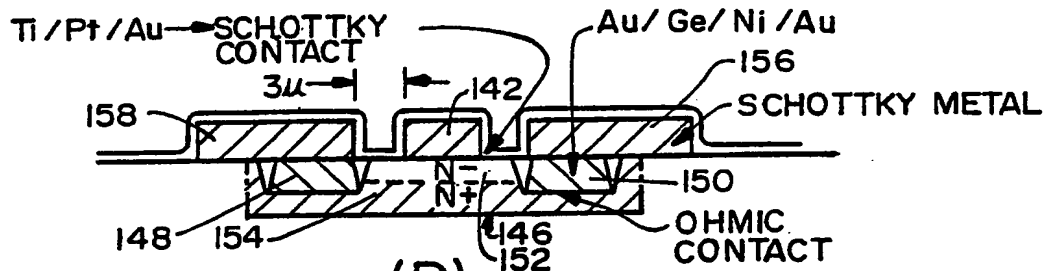
(A)



(B)



(C)



(D)

FIG. 6

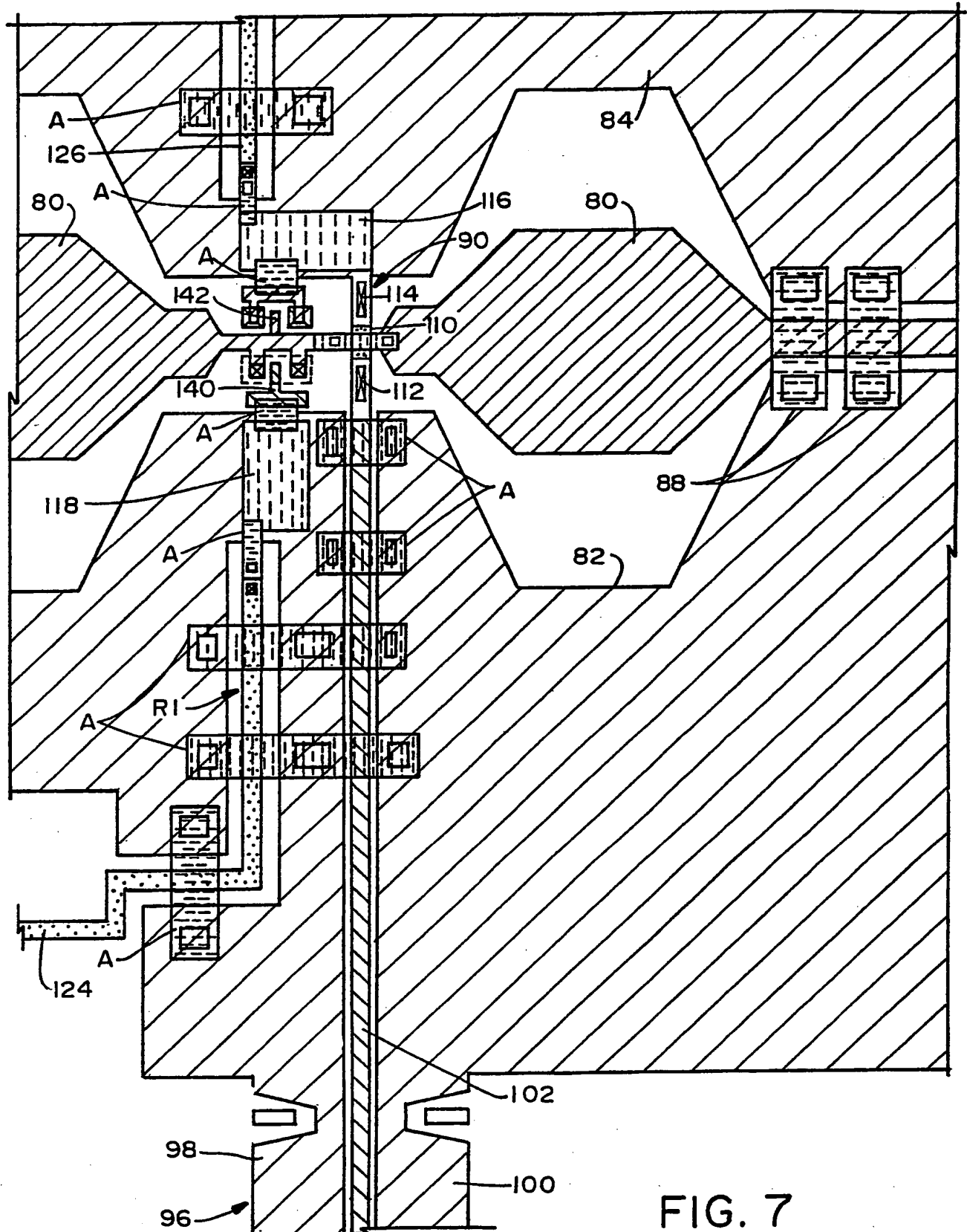


FIG. 7

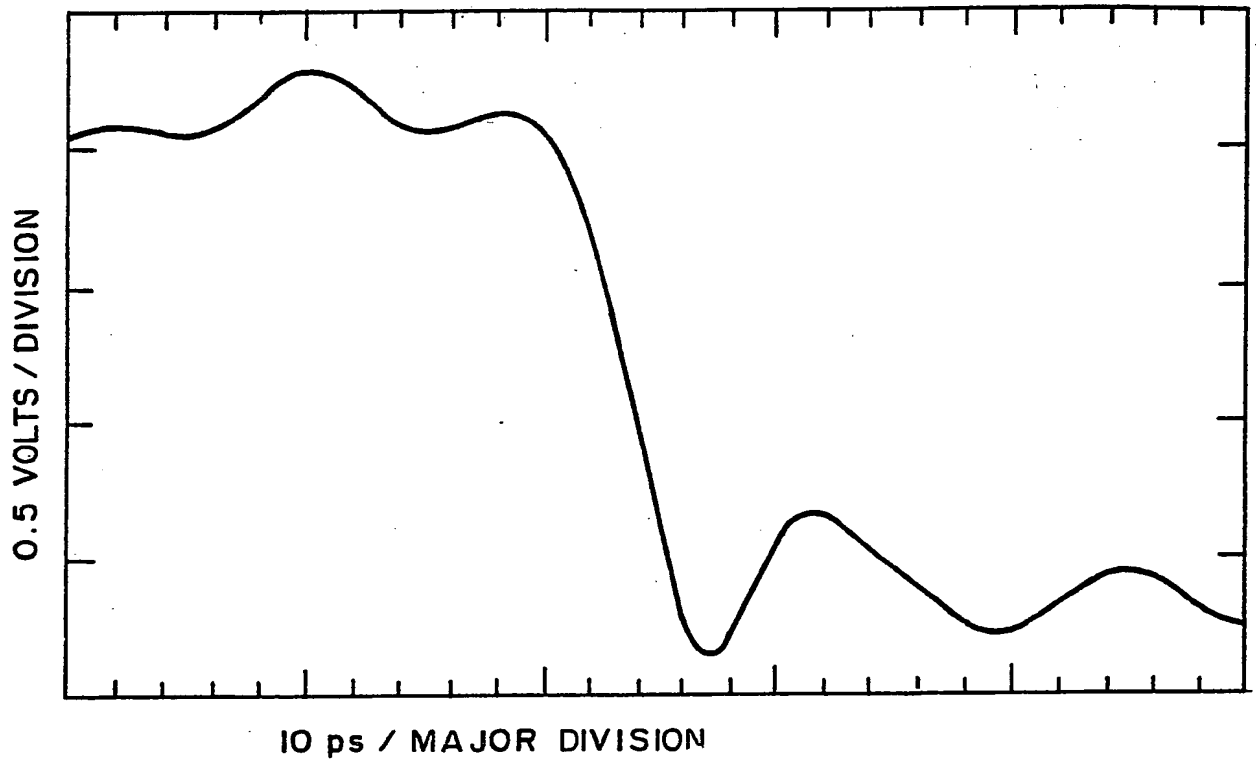


FIG. 8

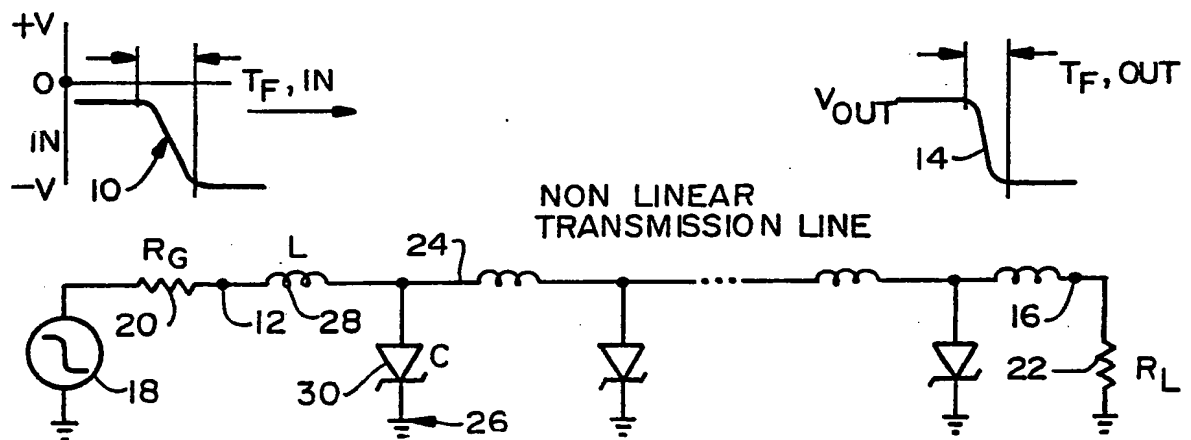


FIG. 9



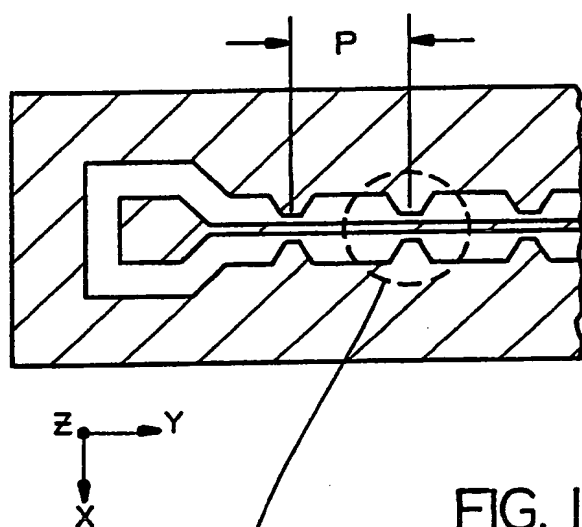


FIG. 12

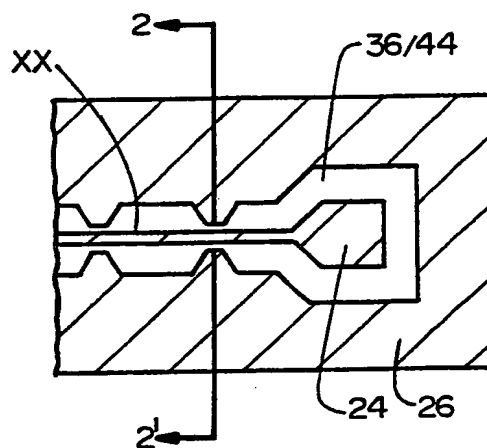


FIG. 13

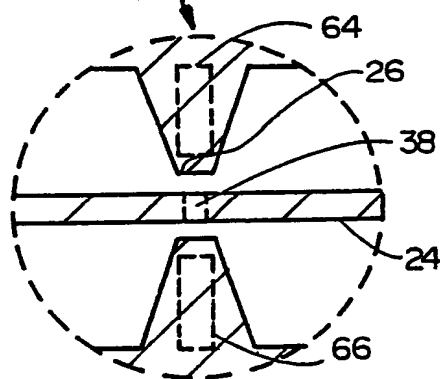


FIG. 14

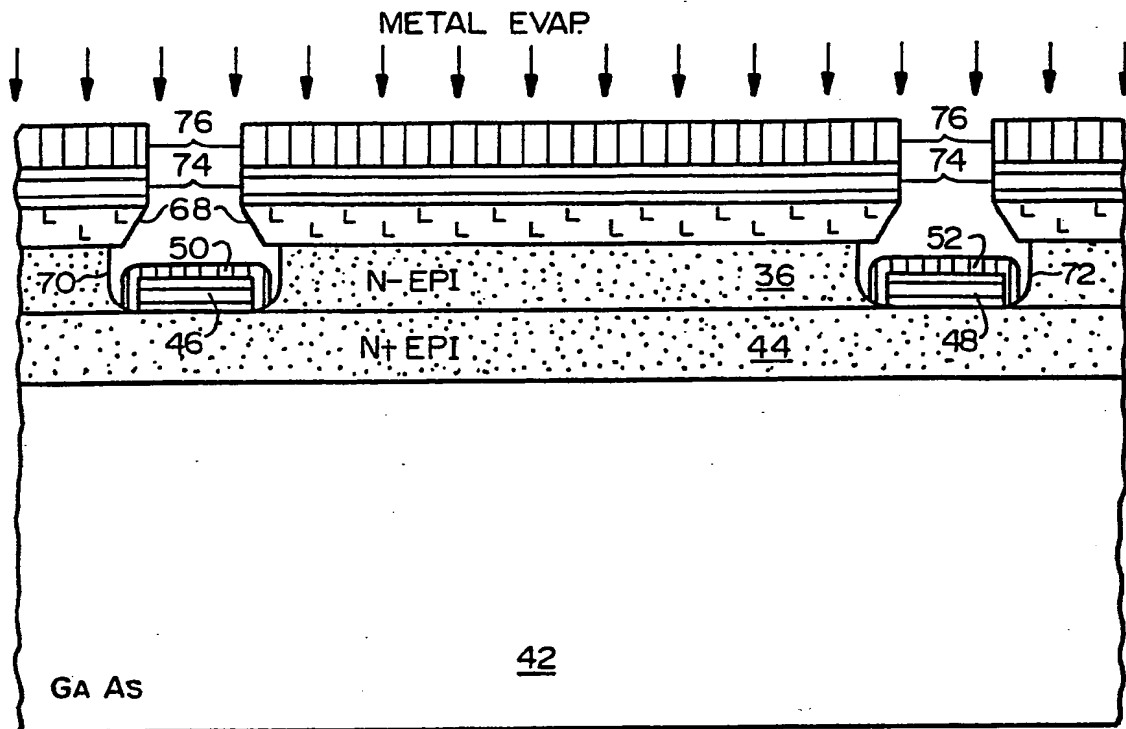


FIG. 15

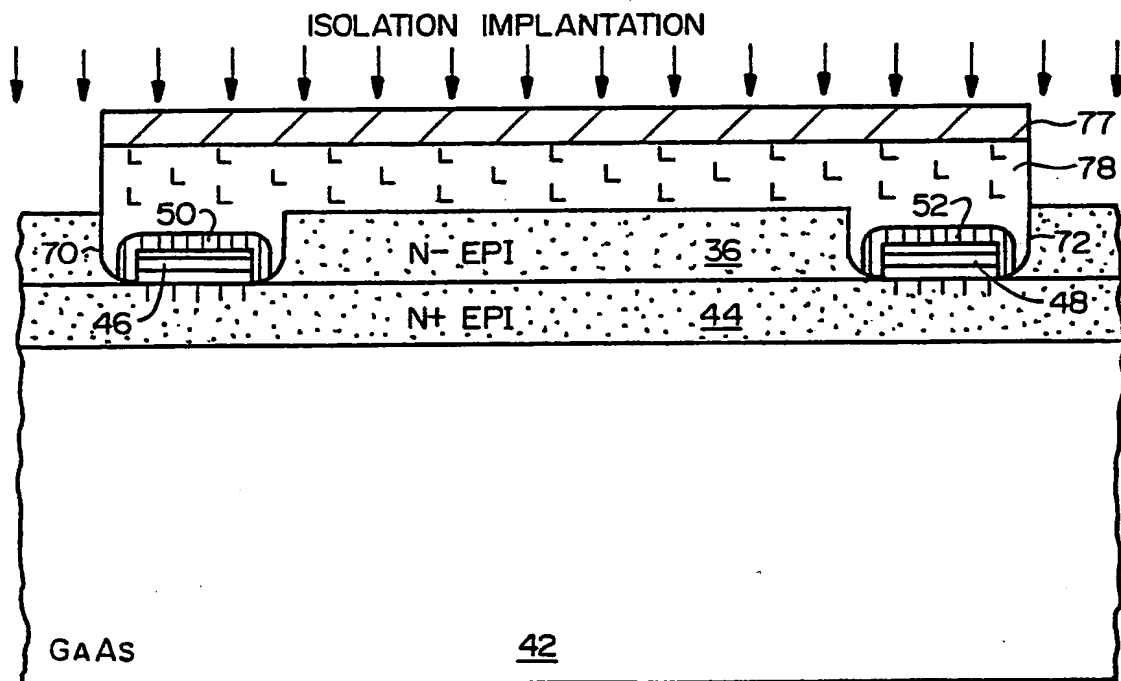
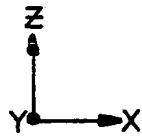


FIG. 16

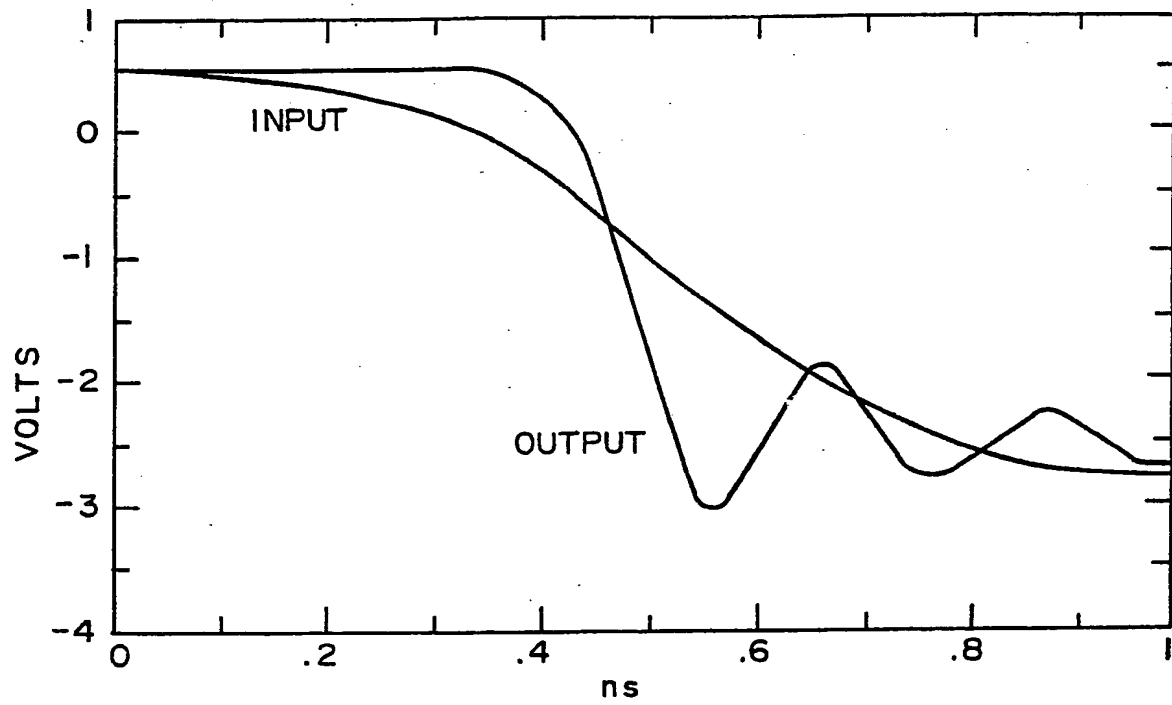


FIG. 17

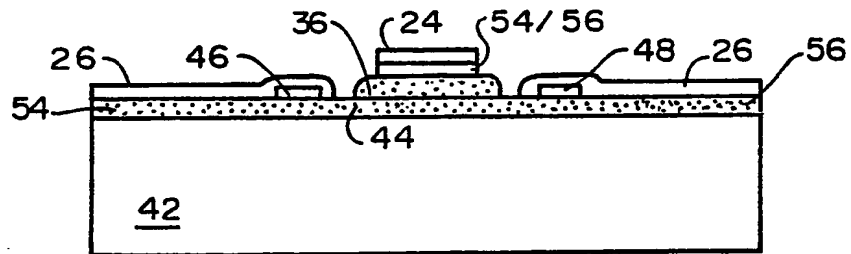


FIG. 18

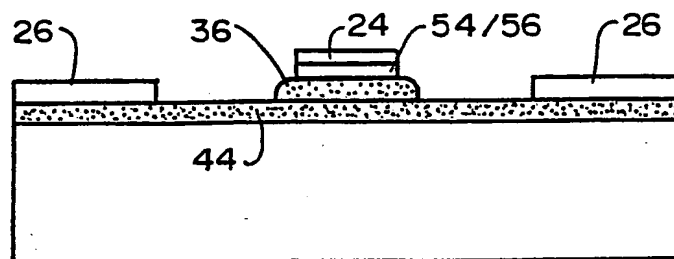


FIG. 19

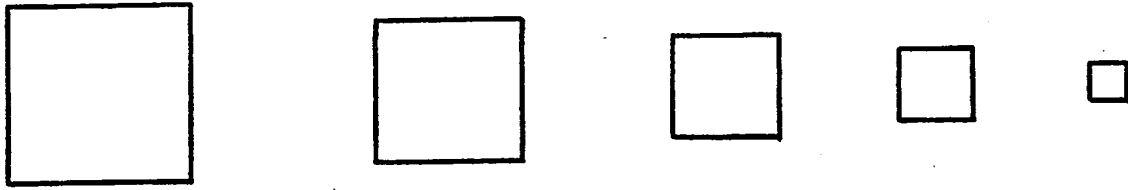


FIG. 20

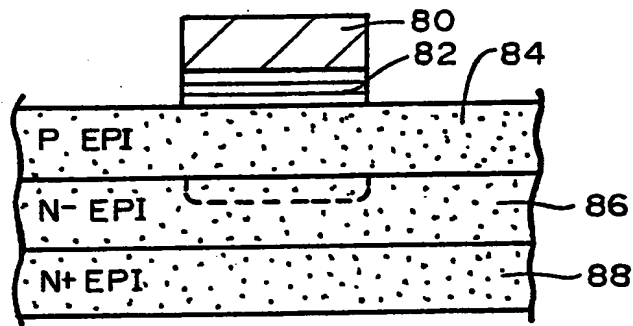


FIG. 21

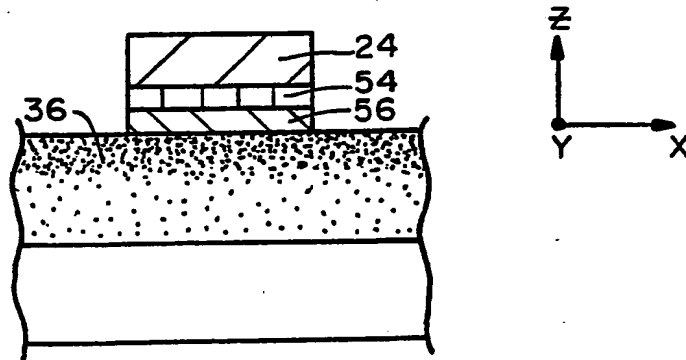


FIG. 22

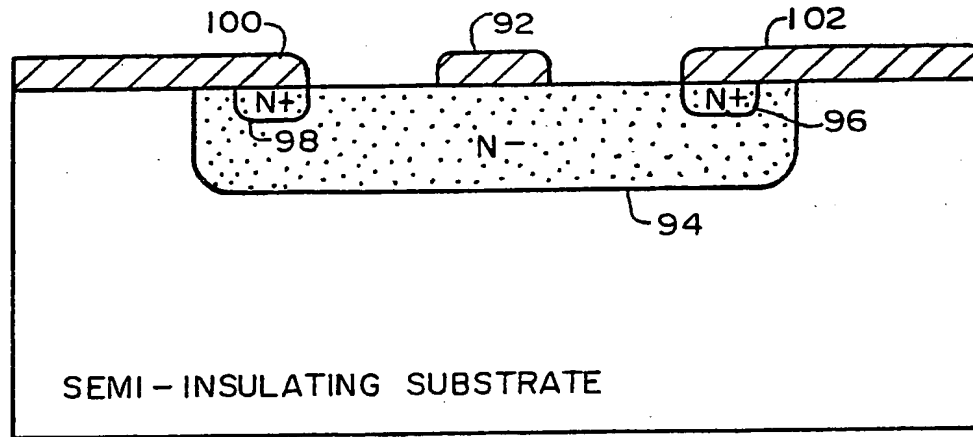


FIG. 23

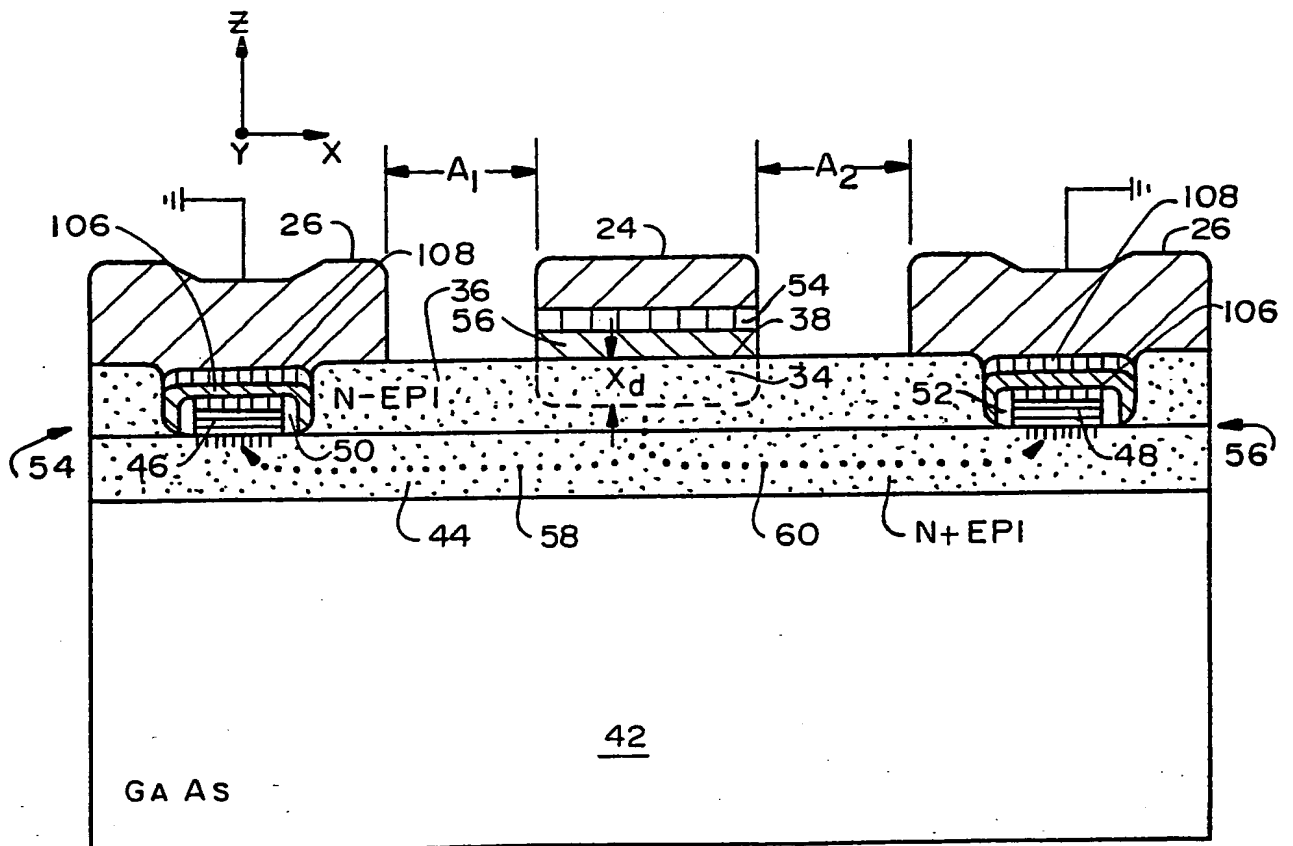


FIG. 24